Distribution and characteristics of supraglacial channels on mountain glaciers in Valais, Switzerland

Holly Wytiahlowsky[1], Chris R. Stokes[1], Rebecca A. Hodge[1], Caroline C. Clason[1], Stewart S.R. Jamieson[1]

[1]Department of Geography, Durham University, Durham, DH1 3LE, United Kingdom

Correspondence to: Holly Wytiahlowsky (holly.e.wytiahlowsky@durham.ac.uk)

Abstract. Supraglacial channels form a key component of glacier hydrology, transporting surface meltwater to englacial and proglacial positions, which impacts ice flow dynamics, surface mass balance and the hydrochemistry of glacial runoff. The presence of supraglacial channels is well-documented on ice sheets using satellite imagery, but little is known about their distribution and characteristics on mountain glaciers because most channels fall below the resolution of freely-available satellite imagery. Here we use high-resolution (0.15 m) orthophotos to identify channels across 285 glaciers in Valais Canton, Switzerland. For the 85 glaciers with supraglacial channels (>0.5 m wide), we mapped 1890 channels and investigate their distribution and characteristics. We find that glacier hypsometry, size and slope are good predictors of drainage density, with glaciers characterised by lower angle slopes (fewer crevasses) and larger ablation areas (high meltwater supply) exhibiting higher drainage densities. The strongest control on drainage density is glacier mean elevation, with glaciers containing a larger portion of their mass at lower elevations producing higher drainage densities. On average, 80% of high order channels run-off supraglacially, with 20% terminating englacially. However, there is marked inter-glacier variability in where channels terminate, with 40% of glaciers containing no englacially-terminating channels, versus 3.5% where all channels terminate englacially. Most channels are slightly sinuous, with higher sinuosities associated with large, high-order channels that are heavily incised and more likely to reactivate annually. This differs to an ice sheet setting where many supraglacial channels terminate in lakes and fewer channels reach the ice margin.

1 Introduction

Glaciers and ice caps are rapidly losing mass rapidly (Wouters et al., 2019; Hugonnet et al., 2021; Tepes et al., 2021; The GlaMBIE Team, 2025) resulting in sea level rise which is anticipated to continue throughout the 21st century and beyond (Bamber et al., 2019; Edwards et al., 2021; Rounce et al., 2023). Glaciers in the lower latitudes (e.g., the European Alps, Caucasus, New Zealand, the USA) are particularly vulnerable to atmospheric warming and may experience complete deglaciation by 2100 under a strong warming scenario (e.g., RCP8.5) (Zekollari et al., 2019; Rounce et al., 2023). In populated mountain regions, these changes will have profound impacts, as glaciers and snowpacks act as vital water towers, supplying 1.9 billion people worldwide who live in or downstream of glacial catchments with crucial freshwater (Carey et al., 2017; Zemp et al., 2019; Immerzeel et al., 2020; Sommer et al., 2020; Hugonnet et al., 2021; Clason et al., 2023). Glacier meltwater responsible for feeding

proglacial rivers is commonly transported to the proglacial margin by supraglacial channels, with these channels forming an important component of the glacial hydrological system. The presence and distribution of supraglacial channels has implications for a range of glacio-hydrological processes as they affect how efficiently meltwater is routed over, through and under glaciers, with the potential to impact on suspended sediment concentrations and hydrochemistry of proglacial rivers. Higher suspended sediment concentrations, for example, pose harm to downstream ecosystems and proglacial reservoirs, with concentrations generally higher if meltwater is routed to the bed (Swift et al., 2002), rather than transported supraglacially. In addition, the presence or absence of channels that route meltwater to the bed directly affects subglacial meltwater supply, which has implications for subglacial water pressure, the onset of subglacial channelisation, and could in turn influence ice motion (e.g., Willis, 1995; Jobard and Dzikowski, 2006; Banwell et al., 2016). Despite the importance of meltwater routing, the controls and patterns of meltwater transport on mountain glaciers remain relatively understudied. Notably, it is not yet fully understood why the channelised flow of meltwater occurs on some glaciers but not others (Pitcher & Smith, 2019).

The term 'supraglacial stream' was first coined in the 1970s and 1980s from observations of channels in Scandinavia and the European Alps (e.g., Knighton, 1972, 1981, 1985; Ferguson, 1973; Hambrey, 1977; Seaberg, 1988), with their morphology often compared to terrestrial streams. However, these early studies only provided small-scale, local observations of channels on individual glaciers. By comparison, a recent revival in supraglacial channel research has primarily focused on large-scale remote-sensing observations of the Greenland Ice Sheet (GrIS) (e.g., Smith et al., 2015; Gleason et al., 2021; Karlstrom & Yang, 2016; Yang et al., 2015, 2016, 2018, 2019, 2020, 2021, 2022), and to a lesser extent, Antarctica (e.g., Kingslake et al., 2017, Bell et al., 2017; Chen et al., 2024). Recent remote sensing techniques for channel detection on the GrIS (e.g., Yang and Smith, 2013; King et al., 2016) have not been applied to mountain environments because the majority of channels are likely to be below the resolution of the highest resolution satellite platforms (e.g., Sentinel-2 (~10 m), WorldView 3 (0.31 and 1.24 m)). As a result, it is not known whether the principles that govern channel formation on larger ice sheets also apply to mountain glaciers. The latter are characterised by typically steeper and more complex topography and tend to have a larger coverage of debris cover in comparison to ice sheet surfaces.

Much remains unknown about supraglacial channel distribution in mountainous environments, but previous research has helped to establish some fundamentals (e.g., Knighton, 1972, 1981; Ferguson, 1973; Yang et al., 2016). Specifically, the formation of meltwater channels is thought to occur when channel incision via thermal erosion exceeds the rate of surface lowering (Marston, 1983). Channel formation is also influenced by the rate of meltwater production and surface topography, with channels tending to form parallel to the steepest ice flow direction (Irvine-Fynn et al., 2011; Mantelli et al., 2015). Surface topography may re-enforce itself, as once an incised channel forms, the higher incision rates may result in an increasingly topographically constrained channel that reactivates annually. On a smaller scale, high concentrations of channels have been suggested to be correlated with high surface roughness (Irvine-Fynn, 2011), while the presence of micro to macro scale surface structures also influences meltwater routing (e.g., Rippin et al., 2015). Where channels occur, they are often reactivated annually depending on their depth, with the most deeply incised channels suggested to be a product of high discharge or high slope (St Germain & Moorman, 2019). However, incised channel profiles are not typically uniform, and most channels commonly exhibit asymmetric cross-profiles due to the dominant direction of solar radiation (St Germain & Moorman, 2019). Additionally, discharge rates are a strong control on channel

morphology, in particular sinuosity, with channels observed to increase in sinuosity throughout the melt season (e.g., Dozier, 1976; Hambrey, 1977; St Germain & Moorman, 2019). Similar to terrestrial river networks, supraglacial channels generally follow Horton's laws, meaning that higher-order channels (i.e., where the highest-order is the main channel) are longer, have lower slopes, and are comprised of a lower number of channel segments (Horton, 1945; Yang et al., 2016). However, much of what we know about supraglacial channels was established from cold to polythermal glaciers or from observations of a small number of individual glaciers (e.g., Knighton, 1972, 1981, 1985; Gleason et al., 2016; St Germain & Moorman, 2019).

In this paper we investigate a range of potential controls on channel distribution and properties for a large sample of glaciers (n = 285) in a region characterised by high melt rates. We use high-resolution (~0.15 m) orthophoto imagery from 2020 to produce the first comprehensive inventory of 1,890 supraglacial channels in a mountain glacier environment, with a focus on Valais Canton, Switzerland. Our aim is to characterise the morphometry of supraglacial channels on mountain glaciers, providing insight into where and why they form. This is important for understanding how mass is transported through and away from glacier, and for determining how uniform surface hydrological characteristics (e.g., channel, channel transport pathways) are between glaciers which is beneficial for informing modelling of glacier hydrology and ice motion. Using GIS software, we extract channel metrics (length, sinuosity, slope, elevation, terminus type, proximity to debris) and glacier characteristics (aspect, size, drainage density, elevation, crevassed extent) which are supplemented by qualitative observations. Using our data, we explore the relationship between glacier and channel characteristics using statistical measures and infer whether glacier surface characteristics can explain the presence or absence of channels.

2 Study location

When compared to many glacierised regions, Switzerland has the largest repository of high spatial and temporal resolution national LiDAR and orthophoto surveys, providing excellent coverage for the mapping of supraglacial channels. We focus on Valais Canton in southern Switzerland which contains 303 glaciers over 0.1 km^2, covering a total area of 545 km^2 in 2015 (Fig. 1; Linsbauer et al., 2021). It is the most glacierised Swiss Canton and in 2015 glaciers in Valais had a mean area of 1.8 km^2, a median of 0.43 km^2 and a maximum area of 77.3 km^2 (Grosser Aletschgletscher) (Linsbauer et al., 2021). We identified Valais Canton as a suitable study site as its glacier size distribution is comparable with Switzerland as a whole, and the glaciers range from shallow to steep gradients, have differing hypsometries (ice area-elevation distributions) and vary in crevasse densities. Thus, this study site captures a wide range of potential influences on channel distributions and characteristics. Valais is comprised of the Bernese Alps to the north and the Pennine Alps in the south, separated by the Rhône Valley (Fig. 1). Glaciers in the Bernese Alps are the largest in the canton and most exhibit a south-to-southeast aspect (mean: 163°). In contrast, the largest glaciers in the Pennine Alps have a north and west aspect (mean: 347°). Glaciers in Valais have an average maximum elevation of 3450 m.a.s.l (min: 2356, max: 4599) and an overall mean elevation of 3091 m.a.s.l (min: 2267, max: 4025).

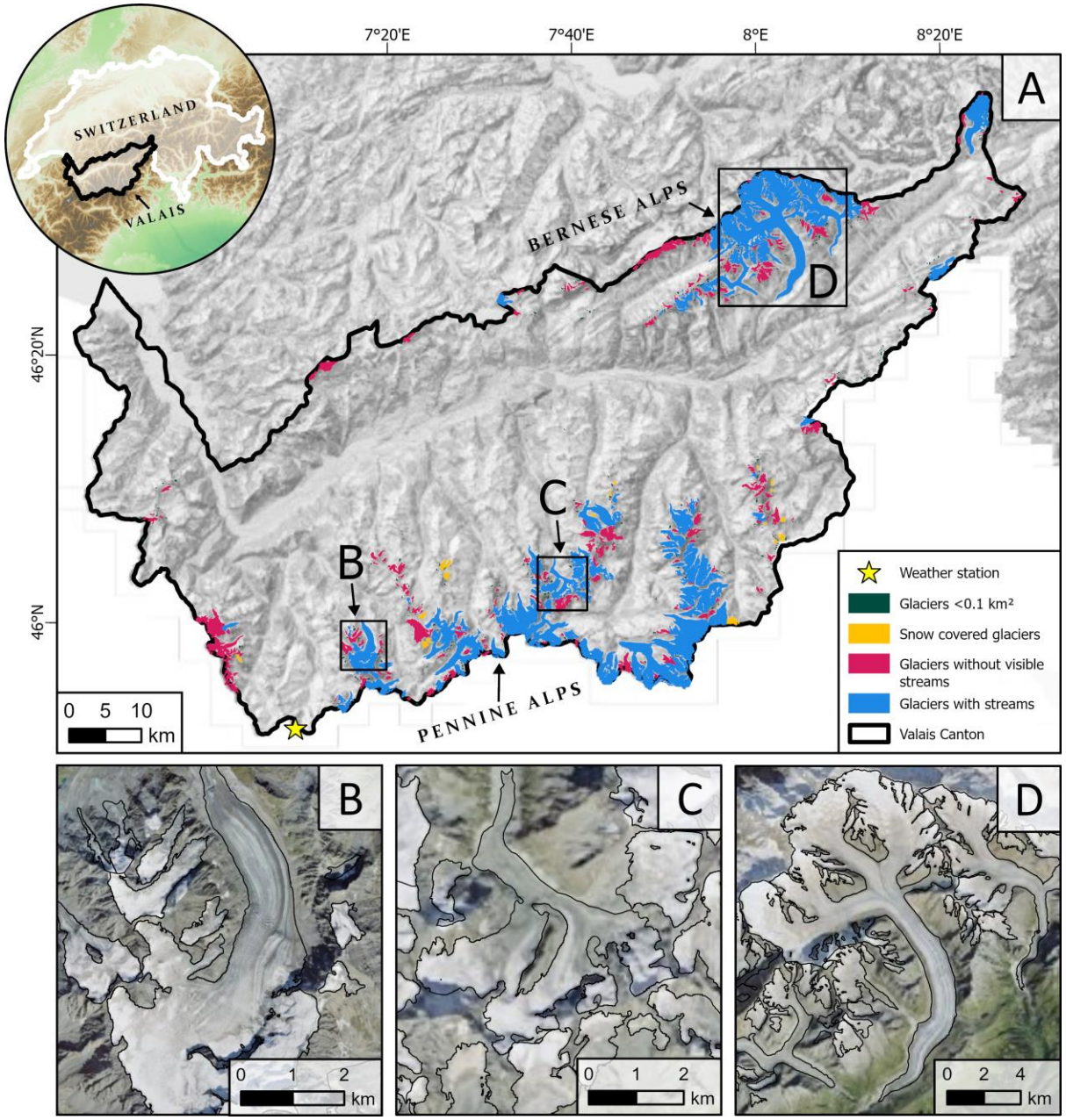

Figure 1: The study site area, which contains 303 glaciers >0.1 km^2. (A) The location of Valais Canton (black) is shown within southwest Switzerland. Glaciers found to contain visible streams (>0.5 m wide) are shown in blue, glaciers without streams (>0. 5 m wide) are in pink, glaciers fully covered by snow are in yellow, and all glaciers <0.1 km^2 (which we omit from this study) are shown in dark green; (B) an example of a large valley glacier, with smaller glaciers at higher elevations; (C) the debris-covered tongue of Glacier du Grand Cornier and surrounding smaller glaciers; and (D) the larger glaciers (e.g., Grosser Aletschgletscher, centre right) in the north of Valais Canton. The location of Col du Grand St-Bernard meteorological weather station is indicated by a yellow star. Glacier outlines used are from the Swiss Glacier Inventory (SGI2016), with glacier extent shown for 2015-16. The outlines are overlayed on basemap imagery sourced from Esri (2024).

Within Valais, the only meteorological station with a similar elevation to many glacier termini is Col du Grand St-Bernard (2472 m.a.s.l) in the Pennine Alps, which (between 1991 and 2020) recorded mean July air temperatures (2 m) of 8.4°C, mean January temperatures of -6.9°C, and mean annual temperatures of -0.1°C. At Col du Grand St-Bernard, July averages 140 mm of precipitation (1991-2020), with 12.7 days a month experiencing > 1 mm of precipitation, compared to a January average of 242 mm across an average of 12.9 days. However, Switzerland's climate is changing and mean air temperatures between 2013 and 2022 were 2.5°C warmer than pre-industrial temperatures (MeteoSwiss, 2024), which has greatly impacted the mass balance of Swiss glaciers in recent decades (Fischer et al., 2015; Davaze et al., 2020).

3 Methods

3.1 Imagery acquisition and channel delineation

The method commonly used for automated channel detection, developed by Yang and Smith (2013) for delineating water bodies on the GrIS from WorldView-2 imagery (1.84 m), involves the application of a normalised difference water index adapted for ice ($NDWI_{ice}$). Following Yang and Smith (2013), we applied a modified $NDWI_{ice}$ approach to a high resolution (0.15 m) orthophoto tile (1 km by 1 km) on the Grosser Aletschgletscher. However, our $NDWI_{ice}$ output predominantly detected water-filled crevasses, and whilst it was able to detect some channels >0.5 m in width, it typically identified only the largest channels (mostly > 1 m). It also missed many channels that were visible but contained very small amounts of water, or incised channels where the water surface was not visible. This method is likely better suited to coarser imagery (less visible crevasses) in less complex terrain and/or for simply using a threshold to extract high order channels. As a result, we undertook manual mapping, which in some instances has been found to be seven-fold more accurate in ascertaining channel density compared to automated methods (King et al., 2016).

We obtained high-resolution cloud-free orthophoto imagery (0.15 m resolution) from SwissTopo (swisstopo.admin.ch), with acquisition dates during mid-July 2020. Imagery was not available for later in the melt season. Hence our data is unlikely to capture the peak extent of channel distribution, which is expected to occur in late summer. Snow conditions at Col du Grand St Bernard (Fig. 1) in mid-July 2020 were likely to be lower than average (2010 to 2020 mean winter total: 704 mm) due to low total winter (December, January, February) precipitation in 2019/20 (2019/20 total: 570 mm). However, May temperatures were slightly warmer than average (2020 mean: 3.4˚C; 2010-20 mean: 1.7˚C), followed by a colder than average June (2020 mean: 4.8 ˚C; 2010-2020 mean: 6.3 ˚C), meaning that whilst there was less snow, it may have melted more slowly than previous years.

Our first procedure was to remove all glaciers in Valais Canton smaller than 0.1 km^2 from our study glaciers (582 reduced to 303 glaciers). This is because they are likely too small to produce large enough channels to be detected by our imagery, and because many small glaciers in the Swiss Glacier Inventory (SGI2016) are unlikely to meet the criteria to be identifiable as glaciers (Leigh et al., 2019). Due to the date of imagery acquisition, 6% of glaciers were still completely snow-covered and were omitted from further analyses as the presence or absence of channels could not be detected, resulting in 285 glaciers remaining in our sample. Within this sample, the mean percentage snow-free glacier area was 38.9% in mid-July 2020, with some variation in snow cover at different elevation

bands. For example, glaciers with a mean elevation between 2500 – 2800 m.a.s.l had a 45.0% snow-free area on average, compared to 36.6% at 3100 – 3400 m.a.s.l. The lowest percentage of snow-free area was 4.9% at a high elevation cirque, and five glaciers were completely snow-free by mid-July but were all under 0.7 km^2.

Each glacier was systematically surveyed for supraglacial channels in *QGIS* (e.g., Fig. 2). Only channels confidently visible at a 1:1,000 scale were delineated for the purpose of consistency, meaning the minimum channel width we delineated was ~0.5 m wide. We solely focus on these larger (>0.5 m) channels because of difficulties in delineating small channels objectively, which include problems with differentiating complex rill networks from structural features (e.g., fractures) and the need for more subjective judgments where channel width may periodically decrease below the pixel width. Whilst we do not map channels below the scale defined above, many of the glaciers likely contain smaller channels (< 0.5 m wide) that are not sufficiently clear enough to map. These channels may still form a key hydrological component of these glaciers, but we cannot reliably quantify their existence, particularly for smaller glaciers, hence we focus on channels >0.5 m wide, which are also likely to carry the bulk of the meltwater. Individual channels were mapped from their downstream end until they were no longer clearly visible or when channels could not be confidently and objectively mapped. When channels have tributaries above the mapping resolution, the main channels were mapped as one segment, continuing up the largest channel at each confluence. Each tributary channel was then subsequently mapped as a new individual segment. Once mapped, each entire channel segment was assigned codes based on its attributes and whether it was on a bare ice or a debris-covered part of the glacier. The location of the channel terminus was assigned for each channel, which includes the following categories: the glacier terminus, moulin, crevasse, lake, the glacier periphery, adjoins another channel, and disappears beyond the resolution (i.e., the terminus is not visible and cannot be confidently inferred).

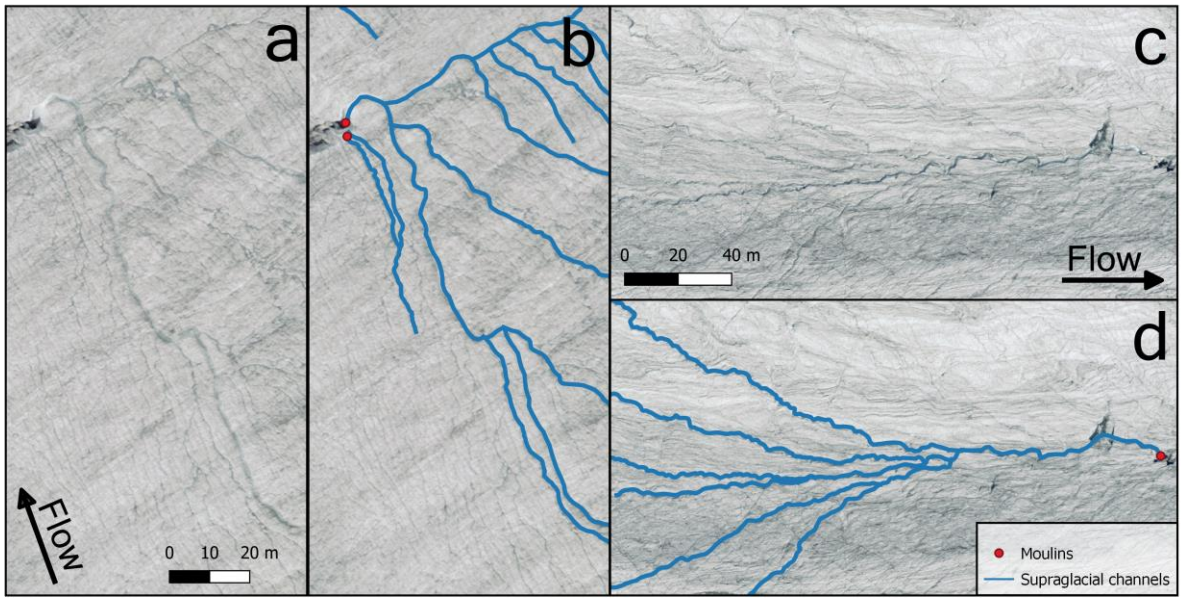

Figure 2: Examples of the mapped output and corresponding orthophoto. Channels are shown in blue, and moulins are represented as red circles when a mapped channel is moulin-terminating. Arrows indicate the direction of ice flow. (a - b) Supraglacial channels on the Glacier de Moiry and (c-d) Allalingletscher. Imagery source: Federal Office of Topography swisstopo.

To ensure consistency, all mapping and the error assessment was conducted by the same individual. We quantified the repeatability of our mapping by delineating channels from the same image of the Rhonegletscher independently months apart. This revealed a 2.6% difference in calculated drainage density and a 0.21% decrease in total channel length from the original mapping (Figure S3). The error from our repeat mapping may have been lower if the mapping has been repeated immediately after the original mapping, whereas the original mapping was conducted consistently over a time period. However, the error margin is small enough to provide a good representation of each glacier's drainage density. Both sets of mapping clearly identify where channels terminate, but the primary source of uncertainty stems from determining when to stop mapping up-channel. We therefore take a conservative approach to avoid over-interpreting channel pathways and only map the up-glacier limit of channels where we are confident that it exists.

3.2 Metrics

A total of 1890 channel segments (polylines) were mapped across 85 glaciers found to contain channels. We then used the high-resolution (0.5 m) SwissALTI3D DEM (2019) from swisstopo.admin.ch (1 sigma accuracy of ± 0.3 m for each dimension) to extract morphometric characteristics from each channel segment. The DEM is coarser than the orthophotos used for channel delineation and there is a one-year offset between their acquisition dates. However, as the DEM is used to calculate larger scale metrics such as elevation and slope, the small offset is unlikely to affect overall results. Channel metrics extracted were segment length, straight line distance, elevation (minimum, maximum), elevation difference and channel slope. The start and end point of each segment were then used to derive the sinuosity of each segment (channel length/straight line distance) and drainage density for each glacier (total length of channels/glacier area). We use the glacier snow-free area at the time of mapping to calculate drainage density, which results in a higher value that if the entire glacier area was used.

Glacier characteristics were obtained from the Swiss Glacier Inventory (SGI2016), which provided information on glacier area, aspect, and elevation (minimum, maximum and mean) in 2015 (Linsbauer et al., 2021). This record is used as it is the most up-to-date record of Swiss glacier area, but glaciers have since undergone substantial recession. The values for glacier slope from the SGI2016 cannot be used as they encompass the whole glacier, whereas for our analysis we wanted to measure the slope of the snow-free portion of the ablation area at the time of channel mapping. To calculate slope values, each glacier polygon was clipped to its snow-free area, and then zonal statistics in *QGIS* were used to extract the mean, minimum and maximum slope value from the SwissALTI3D DEM for each polygon. The snow-free slope value is the only glacial slope value used in data analyses. Upon completion of mapping, we assigned codes to each glacier based on the extent of debris cover and crevassed area due to their potential controls on channel formation. Glacier debris cover is visually estimated and allocated to one of five classes (none, <10%, 10-25%, 25-50% and >50%) and crevassed area is assigned to one of three classes little to none (less than 10% of the ablation area), moderate (10-50% covered), and heavily crevassed (covers >50% of the ablation area).

3.3 Statistical tests

To determine whether there is a relationship between channel morphometry and glacier characteristics, we produced a correlation matrix using Spearman's rank correlation (ρ) (e.g., St Germain & Moorman, 2019). Each metric used in this analysis comprises 1890 values, each representing an individual channel segment. The analysis used the following channel variables: segment length, channel slope, sinuosity, minimum elevation, maximum elevation and elevation range, and the following glacier variables: drainage density, glacier area, mean slope of the snow-free area, aspect, glacier minimum elevation, glacier mean elevation and glacier maximum elevation. For each of the glacier variables, all channel segments on the same glacier are allocated the same value. A singular ANOVA test was conducted to determine the significance of the relationship between debris cover and sinuosity as an ANOVA test is best suited to determining if there is a significant difference between different classes of debris cover. We also conducted a Principal Component Analysis (PCA) to determine the relationship between variables and to identify drivers of variance amongst the dataset, with data normalised to aid in identifying patterns within the data.

4 Results

4.1 Glacier observations

The study area contained 285 glaciers with an area over 0.1 km^2 and a snow-free terminus in 2020 (Linsbauer et al., 2021). Of these, 85 glaciers were found to have supraglacial channels above the mapping resolution (~0.5 m). Glaciers with channels (n = 85) have a mean area of 5 km^2 and glaciers without visible large channels (>0.5 m) (n = 200) have a mean area of 0.6 km^2. However, glacier area frequency distributions peak in the 0.1 to 1 km^2 category for both glaciers with and without visible channels (Fig. 3a). All glaciers larger than 5.6 km^2 were found to contain channels >0.5 m (Table 1, Fig. 3a). Where channels are present, glaciers have an overall mean slope of 21° and a maximum mean slope of 43°, with glacier slope being positively skewed towards lower slope values (Table 1, Fig. 3b). By comparison, where visible channels are absent, glaciers are characterised by steeper overall slopes (mean: 28°, max: 45°) (Fig. 3b).

Table 1: A quantitative summary of glacier and channel characteristics.

	Channel Length (m)	Channel Slope (°)	Sinuosity	Drainage Density (km/km^2)	Mean Glacier Slope (°)	Glacier Area (km^2)
Count	1890	1890	1890	85	85	85
Minimum	5.2	0.8	1.0	0	10.4	0.1
Median	152.2	6.3	1.1	1.5	20.6	1.5
Mean	211.7	8.0	1.1	2.4	21.0	5.0
Maximum	4314.4	47.8	3.8	15.3	43.0	83.0
Range	4309.3	47.0	2.8	15.2	32.6	82.9
Standard Deviation	228.3	6.3	0.1	2.6	6.5	10.7
Standard Error	5.3	0.1	0.0	0.3	0.7	1.2
Kurtosis	65.8	7.4	153.0	9.0	1.1	35.3
Skewness	5.5	2.3	9.5	2.6	0.8	5.4

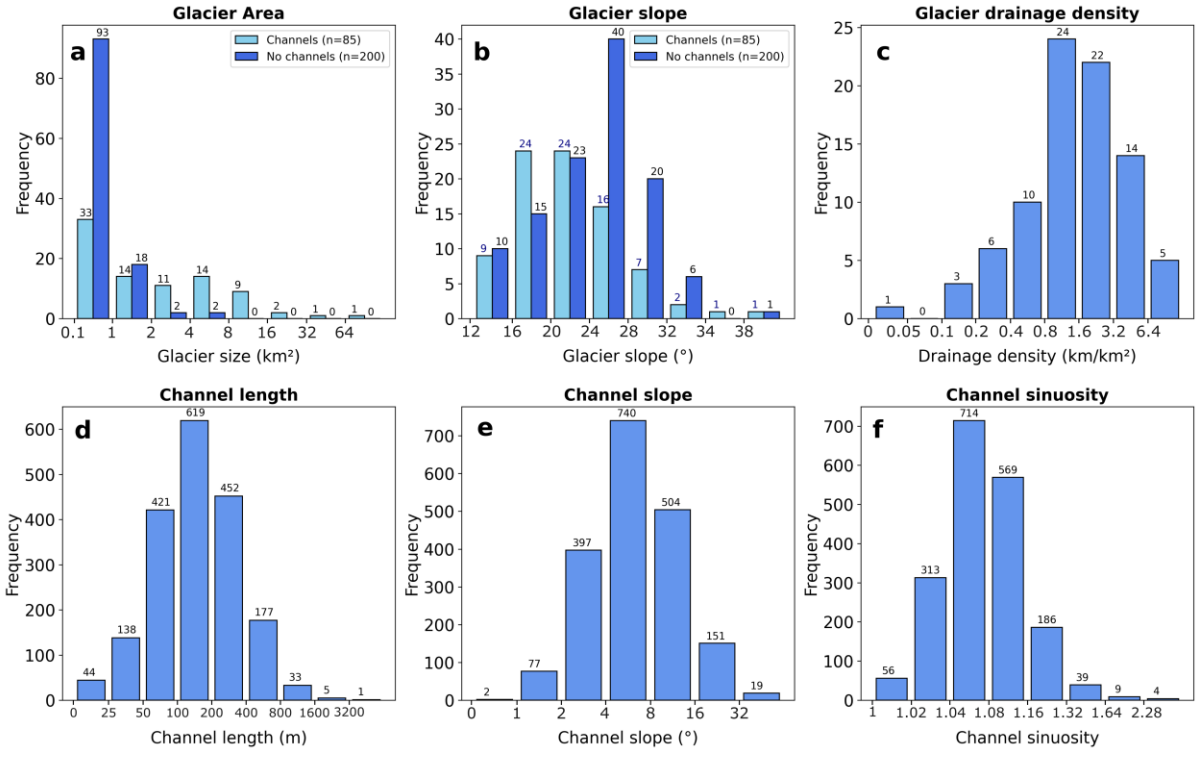

Figure 3: Histograms of extracted metrics. Note that the x-axis is log scale (except for Fig. 3b) and the numbers above each bar represent the number of channels/glaciers within each class. The range shown by each bar is indicated by the x-axis values to either side. The range is exclusive of the lower value, and include the higher one (e.g., >1 - ≤2). (a) Glacier area (km^2); (b) glacier slope (°); (c) glacier drainage density (km/km^2); (d) channel segment length (m); (e) channel slope (°); and (f) channel sinuosity.

Glaciers without large channels (>0.5 m) are more likely to terminate at higher elevations (mean minimum elevation: 2936 m) compared to glaciers with channels (mean minimum elevation: 2797 m), which are often characterised by longer valley glacier tongues. Where glaciers support channels, they are more likely to have a higher maximum elevation (mean maximum elevation: 3637 m) than glaciers without large channels (mean maximum elevation: 3555 m). Where channels >0.5 m are present, there is a mean drainage density of 2.4 km/km^2 and a maximum of 15.2 km/km^2. The latter was found on the Oberer Theodulgletscher, which is situated on a low slope plateau and has the lowest glacier slope angle in the dataset (13°) (Fig. 3c, Fig. 4a). To summarise, glaciers containing channels are larger, have lower mean slopes, and have a larger portion of their area at lower elevations compared to glaciers without large channels (>0.5 m).

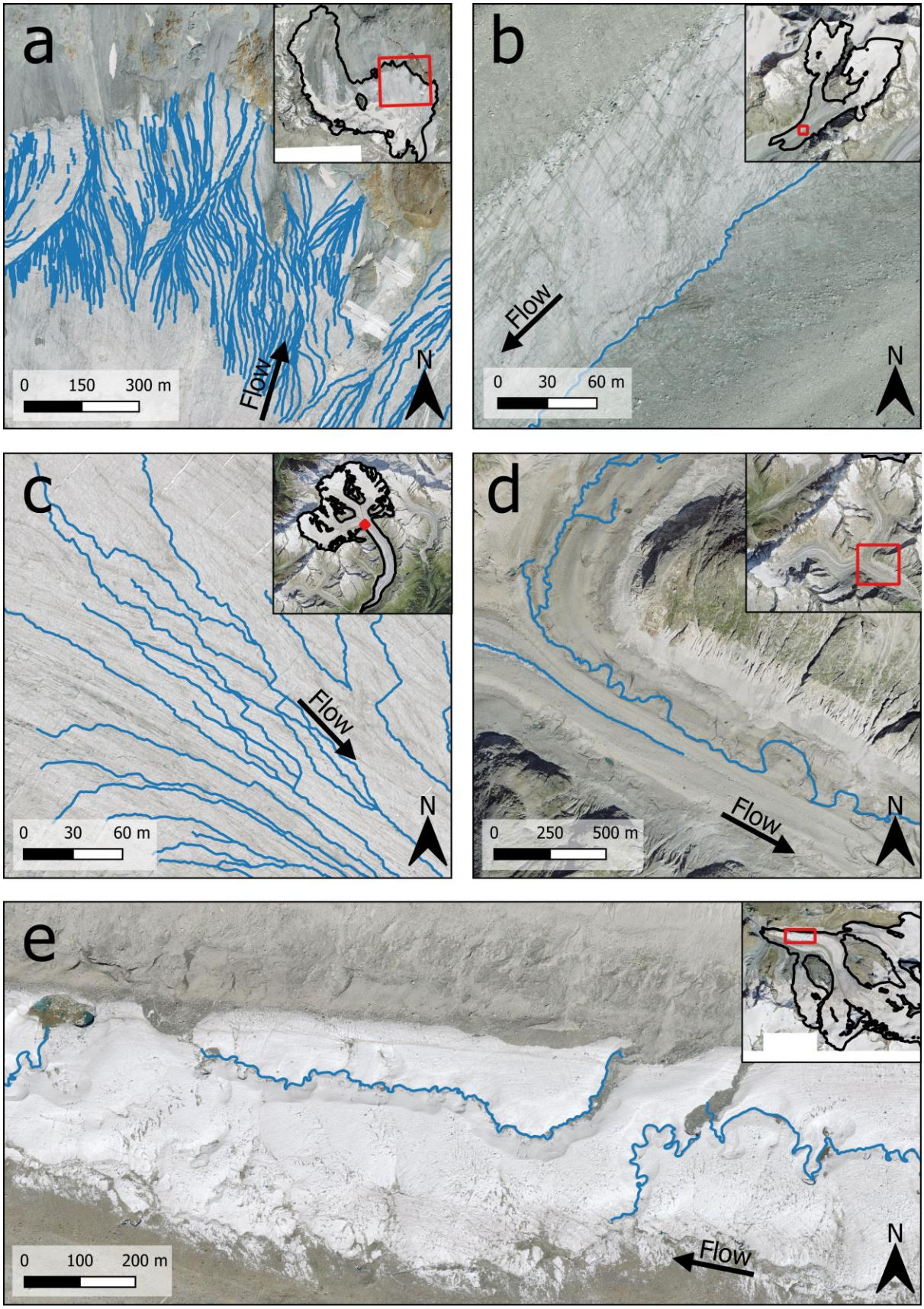

Figure 4: Examples of supraglacial channels. Channel location is shown in relation to the whole glacier in the top left of each panel, with the panel extent shown in red. (a) Channels on the Oberer Theodulgletscher;

(b) a channel at the interface between bare ice and debris-covered ice on Glacier du Brenay; (c) channels on the Grosser Aletschgletscher - note the straight segments where crevasses have been exploited; (d) channels on the debris-covered terminus of the Oberaletschgletscher; and (e) sinuous channels towards the terminus of Gornergletscher, including an example of a channel terminating in a small supraglacial lake (left). Flow indicates the glacier flow direction. Imagery source: Federal Office of Topography swisstopo.

4.2 Channel characteristics

Individual channel segments have a mean length of 212 m, with a positively skewed leptokurtic distribution (Fig. 3d; Table 1). Few segments exceed 1,600 m as the length of most glacier's ablation area is smaller than this value. The channel segments have a mean slope of 8°, and most exhibit a slope between 4 to 16° (Fig. 3e; Table 1). The maximum channel slope observed is 48°, but the overall distribution is positively skewed towards smaller slope values. The sinuosity index of each channel ranges from 1 (straight line) to a maximum of 3.8, with a mean value of 1.1, which is slightly sinuous, but not high enough to be defined as meandering (Table 1). Sinuosity is the most positively skewed variable, with a highly leptokurtic distribution, as most channels are not very sinuous (Fig. 3f).

Channels terminate in a range of settings, with 47% joining another channel, 15% terminating in crevasses, 14% terminating in moulins, 13% disappearing below the mapping resolution, 8% running off at the glacier terminus, 2% running off the side of the glacier, and 1% terminating in a supraglacial lake (e.g., Fig. 4e). When only considering terminal segments (i.e., channels not adjoining another channel or disappearing below the mapping resolution), 72% of segments terminate englacially (crevasses or moulins), 25% run-off (terminus or periphery), and 3% terminate in a supraglacial lake. However, larger glaciers with higher drainage densities disproportionately impact on these values. For example, 582 out of the 1890 mapped channel segments are on the Grosser Aletschgletscher, where no visible channels reach the terminus, hence englacially terminating channels may be overrepresented by a single glacier. Thus, when the channel termini locations at each individual glacier are averaged amongst all glaciers with channels > 0.5 m, 80% of channels reach the terminus supraglacially and 20% of channels terminate englacially. Overall, 48% of glaciers have no englacially-terminating channels, with only 3.5% of glaciers that solely contain englacially terminating channels.

Where visible channels occur, qualitative observations indicate structural and topographic controls on their distribution and morphology. For example, channels often occur at the interface between debris-covered and bare ice (e.g., Fig. 4b), particularly adjacent to medial moraines, where they are confined to a topographic depression, commonly occurring at the confluence between two tributaries. The influence of glacier structure on channel morphology is also observed where trace or shallow crevasses are exploited to produce long, straight channel sections (e.g., Fig. 4c). By comparison, the most sinuous channels tend to occur at lower elevations on large glaciers characterised by larger flat areas towards to their terminus (Fig. 4e).

4.3 Controls on channel morphology and distribution

Here, we investigate links between different supraglacial channel characteristics. Previous studies informed our choice of variables tested for potential relationships, with a focus on how glacier properties (slope, area and elevation) affect glacier drainage density (e.g., Yang et al., 2016) and channel morphology, such as sinuosity and channel segment length (e.g., St Germain & Moorman, 2019). We found that the most sinuous channels are most likely to occur on lower slopes (0 to 10°), with an upper boundary demonstrating that channels on steeper slopes (> 20°) are unlikely to exhibit a sinuosity over 1.3 (Fig. 5a). A relationship between channel segment length and slope is also apparent, with the longest channel segments occurring on the lowest slope angles (Fig. 5b). This relationship is clearly defined by an upper limit where, except for one outlier, channels >500 m are confined to slopes of <20˚ and no channels occur on slopes >50˚ (Fig. 5b). We find no noticeable difference in sinuosity between channels on bare ice and those on debris-covered glaciers (Fig. 5c). However, channels proximal to debris (i.e., channels which are likely to have some sediment content) are more likely to be highly sinuous than channels on bare ice or continuous debris cover, with differences between the classes statistically significant ($p = <0.05$) in an ANOVA test (Fig. 5c). Channel segments that terminate in moulins tend to be the longest (mean: 341 m, max: 1999 m), followed by channels that disappear below the mapping resolution (mean: 259 m, max: 4314 m), and then channels reaching the glacier terminus (mean: 214 m, max: 1193 m) (Fig. 5d). The very few (1%) channels that terminate in supraglacial lakes tend to be short (mean: 109 m, max: 260 m), as do channels that adjoin a higher-order channels (mean: 169 m, max: 1174 m) (Fig. 5d).

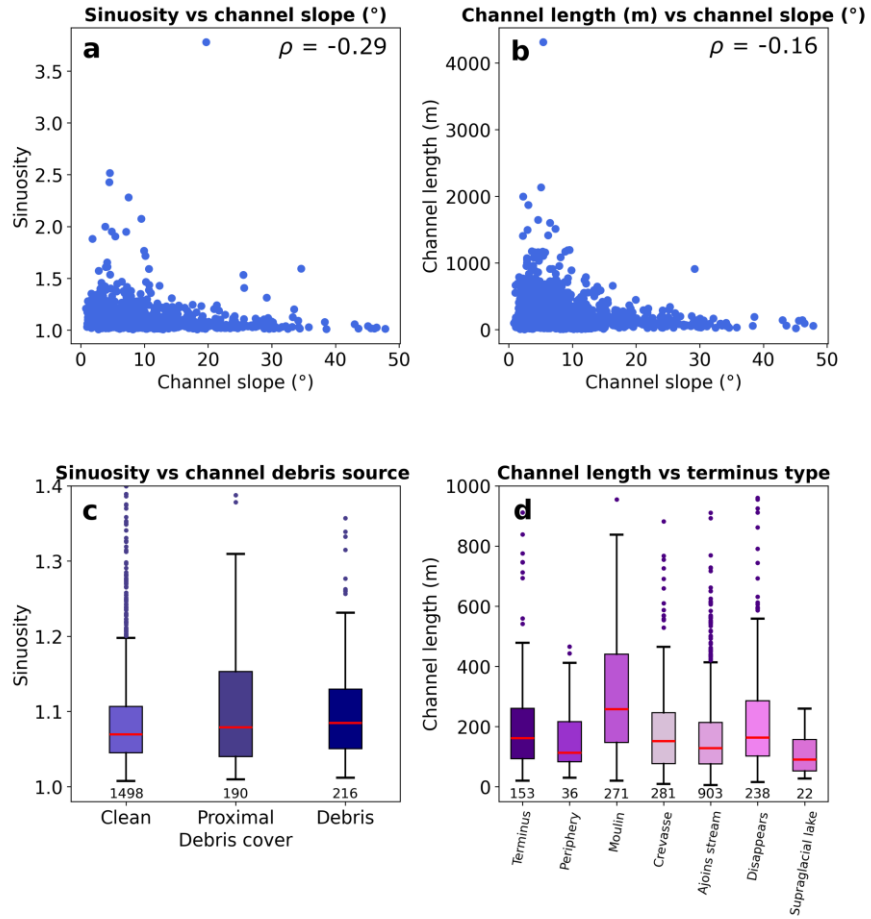
Sinuosity vs channel slope (°)
a
ρ = -0.29
Sinuosity
Channel slope (°)
Channel length (m) vs channel slope (°)
b
ρ = -0.16
Channel length (m)
Channel slope (°)
Sinuosity vs channel debris source
c
Sinuosity
1498
190
216
Clean
Proximal
Debris
Debris cover
Channel length vs terminus type
d
Channel length (m)
153
36
271
281
903
238
22
Terminus
Periphery
Moulin
Crevasse
Ajoins stream
Disappears
Supraglacial lake
Drainage density vs glacier slope (°)
e
ρ = -0.46
Drainage density (km/km²)
Glacier slope (°)
Drainage density vs glacier min elevation
f
ρ = -0.09
Drainage density (km/km²)
Glacier min elevation (m)
Drainage density vs max glacier elevation (m)
g
ρ = -0.39
Drainage density (km/km²)
Max glacier elevation (m)
Drainage density vs crevasse extent
h
Drainage density (km/km²)
27
46
12
None
Moderate
Heavy
Crevasse extent

327

Figure 5: Relationships between channel characteristics (a-d) and glacier metrics (e-h). Plots a-d contains data from 1890 channels, and plots e-h contain data for the 85 glaciers with visible channels. Spearman's rank (*ρ)* values are included for all scatterplots, each of which are statistically significant (p = <0.05*).* (a) Sinuosity vs channel slope (°); (b) channel segment length vs channel slope (°); (c) sinuosity vs channel debris source; (d) channel segment length (m) vs terminus type; (e) drainage density (km/km^2) vs glacier slope (°); (f) drainage density (km/km^2) vs minimum glacier elevation; (g) drainage density (km/km^2) vs maximum glacier elevation (m); and (h) drainage density (km/km^2) vs crevasse extent.

Relationships between glacier metrics (Fig. 5e-h) are less clear than for channel characteristics (Fig. 5a-d), which may be due to the lower number of data points (85 glaciers compared to 1890 channels). However, a moderate negative correlation between drainage density and glacier slope exists, with the highest drainage densities occurring on the lowest surface slopes (Fig 5e). A relationship between drainage density and minimum glacier elevation is less obvious (Fig. 5f), but there appears to be a peak in drainage density between 2600 and 3100 m.a.s.l, which would require further validation from a larger sample of glaciers. By comparison, there is less evidence of a relationship between glacier drainage density and maximum glacier elevation. Likewise, there is no statistically significant relationship is identified between glacier aspect and drainage density (Kruskal-Wallis test: p = 0.61). Additionally, the crevassed extent of a glacier affects drainage density, as increased channel interception prevents the formation of longer channels (Fig. 5h).

4.4 Spearman's rank and principal component analysis

We examined the controls on channel morphology and drainage density by calculating a correlation matrix. We use Spearman's rank correlation (ρ) and significance values (*p*), given that many of our relationships do not appear linear. Additionally, given the large sample size within our dataset and that most p-values are < 0.05, relationships, including weak ones, are significant.

The strongest control on glacier drainage density is identified to be glacier mean elevation ($\rho = -0.66$, $p = \leq 0.001$), with higher drainage densities present when a larger portion of glacier mass exists at lower elevations (Fig. 6), followed by glacier mean slope ($\rho = -0.46$, $p = \leq 0.001$). This is consistent with Fig 5e, with the highest drainage densities observed at glaciers with very low slope angles (e.g.,Oberer Theodulgletscher; Fig. 4a).

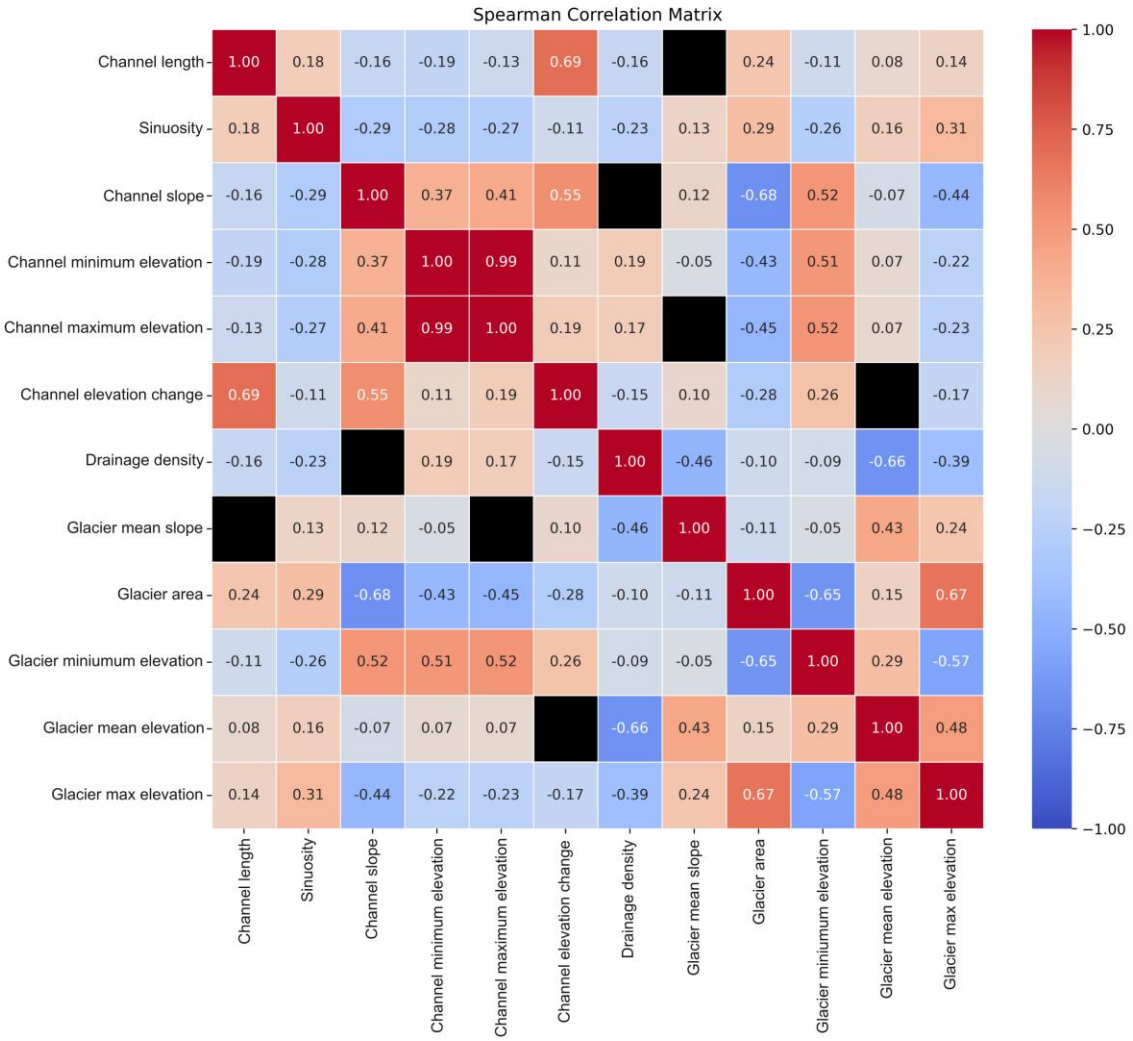

Figure 6: A heatmap matrix of Spearman's rank correlation to show the relationship between glacier and channel characteristics. Correlation values are scaled along a colour ramp and non-significant relationships (p) >0.05 are coloured black.

By comparison, channel morphology is characterised by more complex and weaker relationships between variables. For example, high channel sinuosity can in part be explained by multiple weak correlations: sinuosity values tend to increase with a decrease in channel slope (ρ = -0.29, $p = \leq 0.001$), and the most sinuous channels occur on larger glaciers (ρ = 0.29, $p = \leq 0.001$) with lower minimum elevations (ρ = -0.26, $p = \leq 0.001$) (Fig. 6). Lower angle surfaces are often found when valley glaciers extend down-valley to flatter terrain, supported by observations of highly sinuous channels on low slope glacier tongues (e.g., Gornergletscher) (Fig. 4e). The channel slope is primarily controlled by glacier characteristics, with higher slope channels mostly existing on smaller glaciers (ρ = -0.68, $p = \leq 0.05$), which terminate at higher elevations (ρ = 0.52, $p = \leq 0.05$), meaning the steepest channels are likely to be found at high elevation cirques and hanging glaciers.

To assess the relationship between variables and determine the drivers of variance, we conducted a Principal Component Analysis (PCA). The PCA loadings show that glacier area has a large negative loading on principle

component 1, closely followed by strong positive loadings from minimum glacier elevation and channel elevation (maximum and minimum) (Table S1). By comparison, principal component 2 shows a strong positive loading from drainage density, and large negative loadings from mean glacier slope and glacier mean elevation (Table S1). The first two components explain 50% of the variance within the dataset, with an additional 13%, 12% and 9% explained by principal components 3, 4 and 5, respectively, which together explain 84% of the variability (Table S1). Given the complexity of the dataset, our cluster analysis reveals no clear clustering of data, but the PCA loadings show an expected relationship between elevation variables and slope variables, while drainage density is not closely related to just one other variable (Fig. S2). Overall, our PCA analysis reveals no single, primary driver of variance, instead, it is apparent that there is a complex, yet interlinked relationship between all variables that explain the distribution and appearance of supraglacial channels.

5 Discussion

5.1 Controls on the spatial distribution of channels

Out of 285 glaciers examined within our study area, we find that 85 contain visible channels (>0.5 m) using high-resolution imagery (0.15 m) from mid-July 2020. The presence of channels above our mapping threshold (>0.5 m wide) is primarily controlled by a combination of sufficient meltwater supply and distance for meltwater to coalesce and incise. Hence, in mountain glacier environments, channels >0.5 m are infrequently detected on cirque glaciers due to their smaller ablation area, steeper and often crevassed slopes, and limited distance for meltwater to coalesce. These glaciers may contain channels below our mapping resolution, but these cannot be reliably quantified as part of this study. The glaciers where we observe channels are likely to be larger, resulting in the production of more surface melt. This is supported by the finding that all glaciers in Valais larger than 5.6 km^2 supported channels (>0.5 m) and that glacier area controls much of the variability within the dataset (Table S1) but there is a large variation in drainage density. This variation is in part attributed to glacier slope, which together with ice flow velocity, governs the crevassed area of a glacier which, in turn, controls the area in which channels can form. For example, when crevasses are open, they can intercept meltwater which inhibits the formation of longer channels, whereas crevasses that have closed can add small-scale variability to surface topography and lead to routing of meltwater along crevasse traces. Additionally, channel formation is also governed by glacier hypsometry, with glaciers characterised by a larger portion of their mass at lower elevations more likely to produce higher drainage densities due to a larger ablation area (Fig. 6). It is assumed that we do not capture the maximum channel extent on glaciers with most of their mass at higher elevations due to our imagery acquisition date in mid-July. However, regardless of the date of imagery acquisition, channel density will likely remain highest at lower elevations.

Figure 7 shows a schematic of how the elevation and hypsometry of glaciers is likely to influence the distribution and density of supraglacial channels in alpine settings. The lowest drainage densities are predicted to occur on smaller cirque glaciers due to their lower meltwater supply, restricted distance for meltwater to coalesce into channels, and increased channel inception due to crevasses on often steeper slopes (Fig. 7A). Whilst we detect very few channels >0.5 m on cirques due to our imagery resolution, these glaciers likely still contain smaller channels networks. By comparison, larger valley glaciers (e.g., Grosser Aletschgletscher) tend to exhibit moderate

to high drainage densities because they produce high amounts of meltwater, but much of it may be intercepted by crevasses on steeper slopes, preventing or restricting large channel formation (Fig. 7B). The glaciers with the highest drainage densities are likely to have a large ablation area (high meltwater supply) and occur on lower slopes because fewer crevasses allow large drainage networks to become established (Fig. 6; Fig. 7C). One example of this configuration is the Oberer Theodulgletscher which contains the largest drainage density in our study area (Fig. 4a). It is possible that its high drainage density is also due to its location on a slightly higher elevation plateau, because air temperatures are likely to be cooler than at the terminus of neighbouring glaciers which extend further down valley (Fig. 5f). As a result, the rate of surface lowering is likely lower, meaning that lower rates of incision are needed for channel formation to keep pace with surface lowering, resulting in a higher drainage density (Rippin et al., 2015; Pitcher & Smith, 2019). However, summer temperatures in the Alps are increasing (Sommer et al., 2020), which will result in higher rates of surface lowering, meaning that all glaciers, but more specifically those with larger portions of their mass at lower elevations, will require increased channel incision to counteract the higher rates of surface lowering in order for channels to form. Higher rates of surface melt may, however, counteract this process by increasing the potential for channel incision.

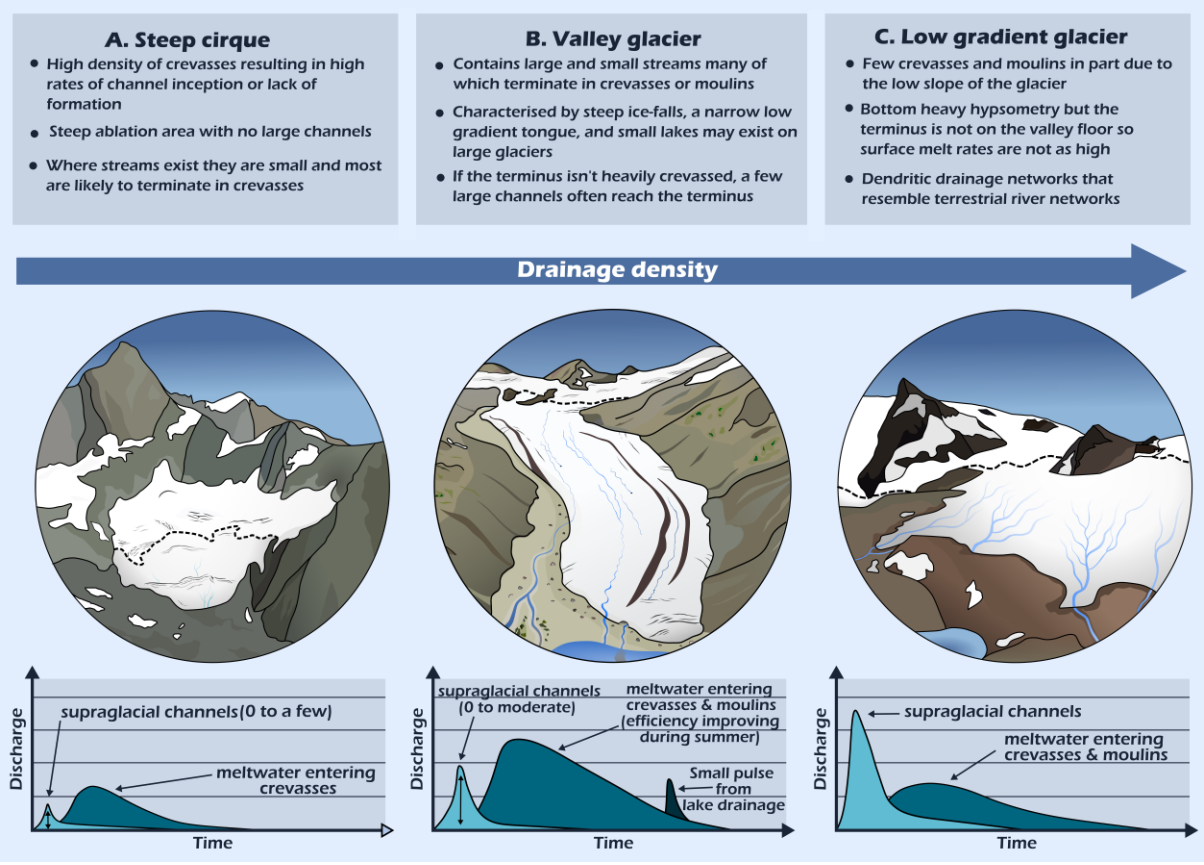

Figure 7: A schematic depicting the range of glacier types (A-C) and their respective characteristics, increasing in drainage density from left to right. Each glacier type corresponds to a hypothesised hydrograph (bottom) depicting changes in proglacial channel discharge over an unknown time period (ranging from minutes to days) as a response to a surface melt event. The hydrographs are hypothesised to represent the general characteristics of each glacier's runoff regime (see text for discussion) and do not

reflect the complexities of individual measured proglacial stream discharge. Light blue shading shows the hypothesised hydrograph if all of the meltwater were to be transported via supraglacial channels, whereas those shown in mid-blue show the hydrograph where the bulk of meltwater is transported englacially/subglacially. Dark blue in panel (b) shows a lake drainage event.

The distribution and density of channels on different types of glaciers is also likely to impact the runoff hydrograph (Fig. 7). Small cirque glaciers (Fig. 7A) are typically characterised by steep, heavily crevassed slopes, meaning meltwater is more likely to be captured by crevasses, and there is limited distance for meltwater to coalesce and form channels. Hence, runoff at cirque glaciers in response to surface melt is likely characterised by a small earlier peak from a few supraglacial channels (light blue shading in Fig. 7A) or a slightly delayed peak as crevasses capture meltwater and route it through the en- (and -sub) glacial system (dark blue shading in Fig. 7A). By comparison, valley glaciers are frequently characterised by larger non-crevassed zones, meaning more meltwater reaches the terminus supraglacially, but channels are often intercepted by crevassed zones or ice falls. This may result in an initial peak from supraglacial channels, followed by a delay in meltwater routed en- (and sub-) glacially (Fig. 7B), with a progressively reduced lag time between melt and peak proglacial discharge throughout the melt season due to increased subglacial drainage network efficiency (Nienow et al., 1998). Additionally, some larger valley glaciers contain small supraglacial and ice marginal lakes (e.g., Gornergletscher and Grosser Aletschgletscher), which may experience infrequent drainage events (e.g., Huss et al., 2007), leading to a sudden peak in proglacial river discharge. Whilst less common in Valais, glaciers characterised by large, low angle ablation areas often contain large supraglacial drainage networks that capture the majority of surface melt. This is because low angle ablation areas typically have smaller and fewer crevasses than most valley glaciers (Fig. 7C). They will tend to have the 'flashiest' hydrograph because the supraglacial drainage network rapidly transfers melt off the glacier surface. Where a small number of crevasses or moulins intercept this drainage, it leads to a more lagged hydrograph response and with a peak well below the hydrograph from supraglacial channel drainage.

Our dataset provides new insight into supraglacial channel distribution across a large range of glaciers, allowing simple inferences to be made about connectivity and possible lag times between melt and peak proglacial discharge based on the locations of our mapped channel termini. Overall, we find that 72% of our mapped highest order channel segments route meltwater to en- or subglacial positions and 25% run off at the glacier margin. However, this varies between glaciers and in the case of the largest glacier, Grosser Aletschgletscher, no mapped channels reach the terminus; attributed to the location of highly crevassed zones forcing meltwater into the glacier (53% of channels enter moulins and 36% enter crevasses). Unlike most glaciers in the Alps, small supraglacial lakes are also present on the Grosser Aletschgletscher, which capture 11% of channels. By comparison, the Oberer Theodulgletscher, which exhibits the highest drainage density within our dataset, contains almost no moulins (2.8% of channel termination) and 27% of channels reach the terminus or periphery. A large number of channels terminate in crevasses on the Oberer Theodulgletscher (70%), but crevasses tend to be small (<0.3 m wide) and it is not known whether meltwater enters englacially or is routed supraglacially through trace crevasses (e.g., Fig 8). Observations have shown that trace crevasses may act as a preferential meltwater pathway, often resulting in channels forming perpendicular to ice flow (e.g., Chen et al., 2024). However, crevasses may also fill with meltwater and be continually overtopped if a channel is situated in a compressive regime, and thus less prone to

hydrofracture (e.g., Chudley et al., 2021). As the true location of channel termination is unknown, our channel segments are always broken at crevasses if a clear pathway cannot be identified.

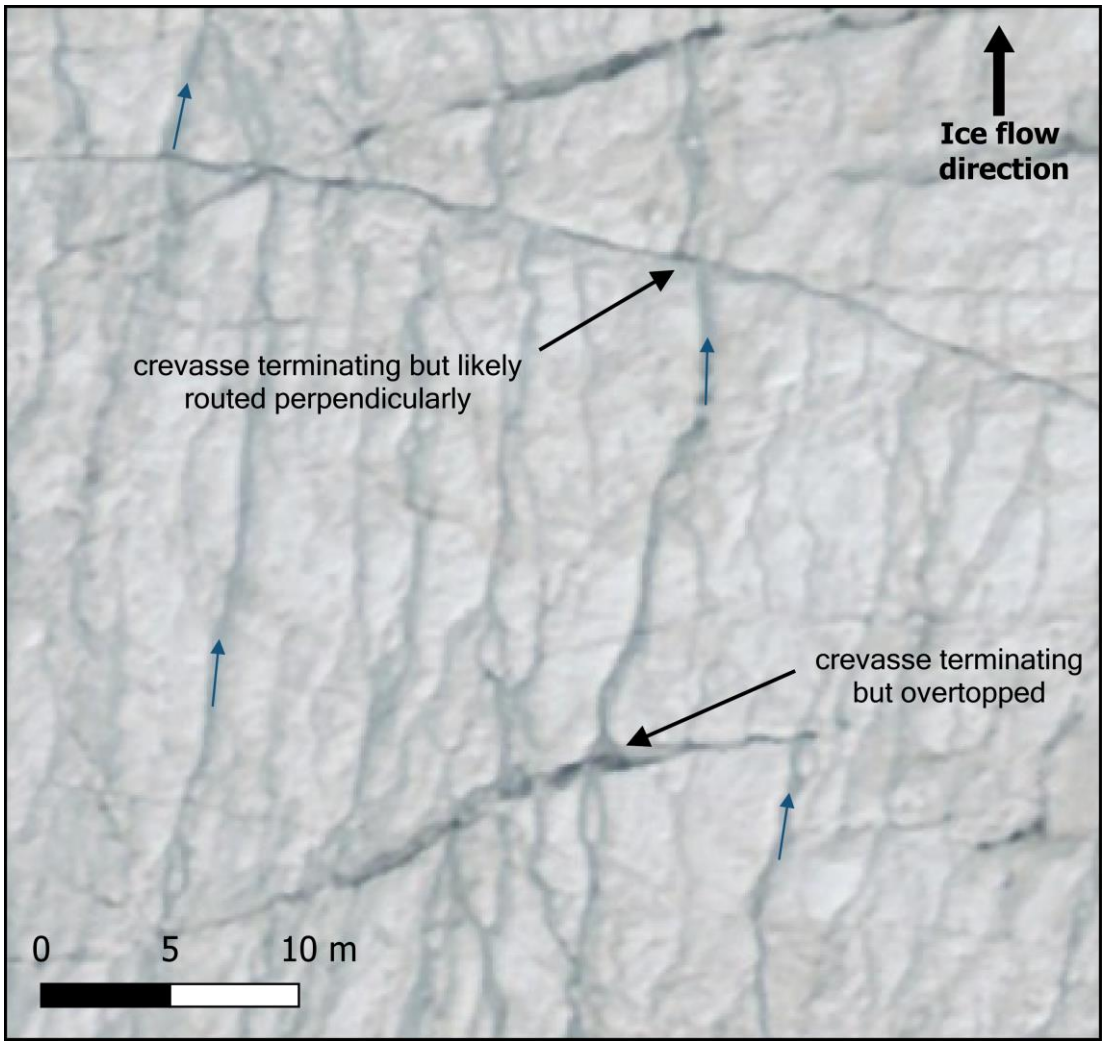

Figure 8: Examples of channels terminating in crevasses on the Oberer Theodulgletscher. Channels are shown to terminate in crevasses but often continue directly down-glacier as some meltwater overtops the crevasse. Small blue arrows indicate the direction of meltwater flow, with meltwater broadly flowing from the bottom to top of the image. Imagery source: Federal Office of Topography swisstopo.

The difference in drainage pathways between the Oberer Theodulgletscher compared to the Grosser Aletschgletscher can be explained by the difference in glacier type outlined in Figure 7, which classifies glaciers based upon their slope and hypsometry. At the Grosser Aletschgletscher, increased meltwater capture by crevasses and moulins likely allows for increased surface-to-bed meltwater transfer, which is supported by observations of its seasonal speed-up in ice flow velocity (Leinss and Bernhard, 2021). Model simulations suggest that increased meltwater presence at the bed increases the excavation of subglacial sediment (Delaney and Adhikari, 2020), which would result in higher proglacial stream sediment concentrations, if streams are not diluted by freshwater flux from proglacially terminating supraglacial channels. This is important for regions such as the Alps because proglacial stream sediment concentrations can directly impact agriculture and hydropower infrastructure

(Micheletti and Lane, 2016). Hence, categorising glaciers based on their slope and hypsometry is beneficial because it provides insight into the anticipated drainage density of a glacier, the likely channel pathways (i.e., sub-/englacially or supraglacially terminating), and whether a higher amount of surface-to-bed meltwater transfer is to be predicted.

5.2 Controls on channel morphology

In Valais Canton, channel morphometry varies significantly between channels, with highly sinuous channels (e.g., Fig. 4d-e) observed to occur on some glaciers but not others. We find that slope affects sinuosity (Fig. 5a); the most sinuous channels are likely to occur on lower angle slopes (0 to 10°) and channels on steeper slopes (> 20˚) are unlikely to exhibit a sinuosity over 1.3. Our observations find that wider and more incised channels (which are likely to have higher discharge) tend to be more sinuous (e.g., Fig. 4d-e). The importance of discharge as a control on sinuosity is supported by St Germain & Moorman (2019) who attribute higher channel sinuosity to increased channel discharge on glaciers in the High Arctic. They also find that channels on higher angle slopes tend to be more sinuous, which is not observed for channels in Valais (Fig 5a). Similarly, higher slopes have been found to increase supraglacial channel incision (Gulley et al., 2009), which based on our observations of high sinuosity channels being deeply incised in Valais suggests that incision (from either slope and/or channel discharge) is needed for the production of highly sinuous channels. These channels are likely to continue to evolve inter-annually due to their incised depth. Given this, we suggest that the relationship between slope and sinuosity in Fig. 5a represents the conditions under which large channels can form (i.e., flatter, less crevassed regions) rather than the direct impact that slope has on sinuosity. This differs to the High Arctic glaciers observed by St Germain & Moorman (2019) where slope is a clear control on channel sinuosity. We attribute this difference to the cold-based High Arctic glaciers typically being less crevassed, resulting in a larger viable area for channel formation (i.e., not solely restricted to smaller, flat, less crevassed zones), and because incision to a deeper depth is likely aided by lower rates of surface lowering.

Our mapping also reveals some distinct differences in appearance and sinuosity between clean and debris covered glaciers in Valais. Channels that have a proximal debris source and those that run directly through debris cover tend to be more sinuous than channels on clean ice (Fig. 5c), with a statistically significant difference between the classes ($p = <0.05$ in an ANOVA test). Figure 4d shows large meandering channels on a debris covered glacier (Oberaletschgletscher), with channels on clean glaciers not being as sinuous. On debris-covered glaciers, we commonly observe less sinuous channels at higher elevations with less debris cover. These less sinuous channels are then funnelled through areas of bare exposed ice until reaching continuous debris-cover where large meandering planforms begin to develop. These channels are anticipated to transport the majority of glacier surface melt as there is a general absence of visible small channels on debris-covered glaciers in Valais, and meltwater transport within the debris matrix is slow and dispersed (Fyffe et al., 2019). Due to high channel incision, some of these debris-covered glaciers (e.g., Fig. 4d) have exposed channel banks of bare ice which are too steep to support debris cover. The exposure of non-insulated ice by channel incision likely exacerbates meltwater production and channel discharge, furthering channel development (e.g., Mölg et al., 2019). Additionally, the

increased sediment presence within channels, which would be expected on highly debris-covered glaciers, may also support channel development. Whilst previous research has documented channels on debris-covered glaciers in mountain glacier regions (e.g., Benn et al., 2017), there has been limited assessment of the effect of debris within supraglacial channels on channel morphometry. This remains poorly understood as most supraglacial research has occurred on ice sheets, where areas of lower albedo are controlled by the presence of, dust, black carbon, algae, and cryoconite deposits (e.g., Ryan et al., 2018; Leidman et al., 2021; Khan et al., 2023).

Further insight may be gained from bedrock rivers, which contain a mixture of sediment cover and exposed bedrock. In bedrock rivers, sediment was found to increase channel erosion rates and increase sinuosity, but high sediment supply may reduce erosion due to producing sediment cover which protects the bed from erosion (Moore, 1926; Shepherd, 1972; Turowski, 2018). Ultimately, future work is needed to determine the role of debris in supraglacial systems, specifically in situ measurements of debris content in channels to determine how it affects channel properties.

5.3 Comparison between mountain glaciers and ice sheets

Previous research has predominantly focused on ice sheet settings (e.g., Smith et al., 2015; Karlstrom & Yang, 2016; Yang & Smith, 2016; Yang et al., 2016, 2021, 2022), hence it is important to establish how comparable channels on ice sheets are to those on mountain glaciers. Similarities in drainage patterns are observed between the two environments, for example, in Valais larger glaciers often contain dendritic drainage patterns (e.g., 4a), which is commonly observed in an ice sheet setting (e.g., Yang et al., 2016, 2019). However, in Valais some glaciers contain parallel, less interconnected networks because there is likely not sufficient distance for meltwater to coalesce. It would be expected that given sufficient distance for meltwater to coalesce, these networks would be comparable to networks on ice sheets, which broadly follow Horton's laws i.e., mean river length increases with channel order and mean slope decreases with channel order (Yang et al., 2016). On a smaller scale, ice surface structures (e.g., trace crevasses and flow-stripes) have been found to exhibit a strong control on meltwater routing in both glaciers in Valais and on ice sheets, meaning that channels do not always follow the steepest path over the ice surface (e.g., Figs. 5c & 9; Chen et al., 2024).

Some differences exist between ice sheets and glaciers in Valais, such as debris may play a larger role in channel formation in mountain environments. For example, channels have been observed to form parallel to medial moraines due to topographic confinement, and debris creates an uneven albedo and higher surface roughness which may increase channel density (Rippin et al., 2015). Glaciers in Valais also exhibit notable differences in coupling between surface melt and the englacial/subglacial system compared to the SW GrIS. On the SW GrIS, virtually all higher-order channels are observed to terminate in moulins (Smith et al., 2015), whereas in Valais 72% of highest order channels terminate englacially (37% in crevasses and 35% in moulins). Additionally, there is a general absence of supraglacial lakes in Valais, except for small lakes on Gornergletscher and the Grosser Aletschgletscher, whereas they exist in abundance on the GrIS (Chu, 2014). On the GrIS, supraglacial lakes act as temporary storage, with the potential for meltwater to refreeze rather than reaching the terminus each melt season; however, hydro-fracture events can cause rapid lake drainage, which has been linked to ice speed-up events (e.g., Das et al., 2008; Morriss et al., 2013; Chudley et al., 2019). In mountain glacier environments, the

general higher surface slopes and absence of temporary supraglacial storage means that proglacial discharge is more clearly linked to rates of surface melt, with few sudden pulses of increased discharge except for in regions prone to glacial lake outburst floods (e.g., High Mountain Asia).

5.4 Future evolution of supraglacial channel systems

The role of climatic warming on supraglacial drainage networks is unclear, but we suggest that supraglacial drainage networks will develop and expand to higher elevations due to rising equilibrium lines (Leeson et al., 2015). Whether discharge in current channels will increase or decrease is dependent on the rate of glacier retreat and summer melt. It is likely that larger glaciers will see an increase in channel discharge due to rising equilibrium lines and subsequent higher rates of surface melt (St Germain & Moorman, 2019). However, the reduction in area for smaller glaciers may be large enough to prevent the formation of established drainage networks, and changes in glacier slope may result in a reconfiguration of the drainage system (e.g., new crevasses may intercept channels that formerly reached the terminus) or a reduction in drainage density (Fig. 5e). Additionally, glaciers in mountain glacier environments are undergoing an increase in debris cover (e.g., Glasser et al., 2016; Fleischer et al., 2021), and it is not fully understood how changes in debris cover will affect surface meltwater supply and transport, channel morphology and surface albedo (e.g., Leidman et al., 2021). Future research would benefit from the growing repository of high-resolution orthophoto surveys to inform our understanding of supraglacial hydrology outside of ice sheet settings, particularly concerning seasonal and interannual channel evolution to better inform modelling of glacier hydrology. It is not currently known how widely applicable our research is to regions with larger glaciers and lower rates of surface lowering (e.g., the Arctic) so future studies may benefit from assessing their similarity. Lastly, further in-situ measurements would be beneficial to determine whether the channels delineated as part of this study represent the majority of meltwater transport on mountain glaciers, or whether channels below our mapping resolution also play a key role in meltwater transport.

6 Conclusion

This study presents the first comprehensive dataset on the distribution and characteristics of supraglacial channels at a regional scale in a mountain glacier environment. We mapped 1890 channel segments >0.5 m wide on 85 glaciers found to contain channels above our mapping resolution in Valais Canton, Switzerland, out of a total sample of 285 glaciers. We found large variability in channel drainage densities between glaciers, with the highest drainage densities on glaciers characterised by low slopes, with a large portion of their area at lower elevations (Fig. 7). The presence of channels is primarily dictated by a sufficiently large supply of meltwater (i.e., large enough glacier area) and an uninterrupted distance for meltwater to coalesce (i.e., absence of crevasses and low ice surface slopes). The primary control on channel distribution is surface topography, with the slope and size of the ablation area providing a clear limit on both where channels can form and their total length (Fig. 5b). However, strong structural controls on channel distribution exist, for example, trace crevasses have been observed to act as preferential meltwater pathways, resulting in channels forming perpendicular to ice flow. Channels also commonly form parallel to moraines due to topographic confinement. Most channels are characterised by low

sinuosity (Fig. 5a), with a general absence of the canyon-like channels described on cold or polythermal glaciers. However, some highly sinuous channels exist, particularly on debris-covered glaciers characterised by channels with steep ice cliffs and on low slope termini, with sinuous channels most commonly occurring where channels are also deeply incised.

Glaciers in Valais are characterised by a large proportion of channels reaching the glacier margin rather than terminating englacially. When the channel termini locations are calculated per glacier, the average glacier would have 80% of its channels run directly off the glacier while 20% would terminate englacially. Overall, 48% of glaciers contain no englacially terminating channels, compared to only 3.5% of glaciers where all channels terminate englacially. The location of channel termini (i.e., supraglacial or englacial) is hypothesized to produce different hydrograph responses to surface melt, some of which we suggest may be more common for certain glacier hypsometries. The observed channel terminus locations in Valais differs from typical ice sheet settings where very few supraglacial channels reach the ice margin, with most surface melt transported englacially through crevasses or moulins. In comparison to ice sheets, channel drainage networks in mountain glacier environments are often less established due to glaciers having smaller drainage areas and there being less distance for channels to coalesce, with valley glaciers often narrowing down-glacier reducing the possible size of drainage networks.

7 Supplementary Data

Table S1: The eigenvectors for principal components 1 to 6 from a PCA analysis of glacier and channel characteristics, with PC1 being the most significant. The three largest loadings for each principal component are in bold.

	PC1	PC2	PC3	PC4	PC5	PC6
Glacier area	**-0.439**	0.042	0.034	0.288	-0.187	0.054
Glacier minimum elevation	**0.435**	-0.112	0.085	-0.098	**0.407**	-0.178
Channel maximum elevation	**0.393**	0.159	0.066	**0.436**	-0.115	0.186
Channel length	-0.070	-0.264	**-0.582**	0.312	0.195	**-0.199**
Channel minimum elevation	0.382	0.196	0.121	**0.423**	-0.100	0.196
Channel sinuosity	-0.117	-0.182	-0.122	-0.041	**0.468**	**0.845**
Channel elevation range	0.166	-0.345	**-0.542**	0.198	-0.173	-0.068
Channel slope	0.320	-0.203	-0.066	-0.115	**-0.483**	**0.255**
Drainage density	0.131	**0.543**	-0.268	-0.009	0.041	0.083
Mean glacier slope	0.119	**-0.439**	0.136	-0.309	-0.335	0.141
Glacier mean elevation	0.170	**-0.376**	**0.401**	0.280	0.339	-0.188
Glacier max elevation	-0.330	-0.175	0.264	**0.462**	-0.163	0.086

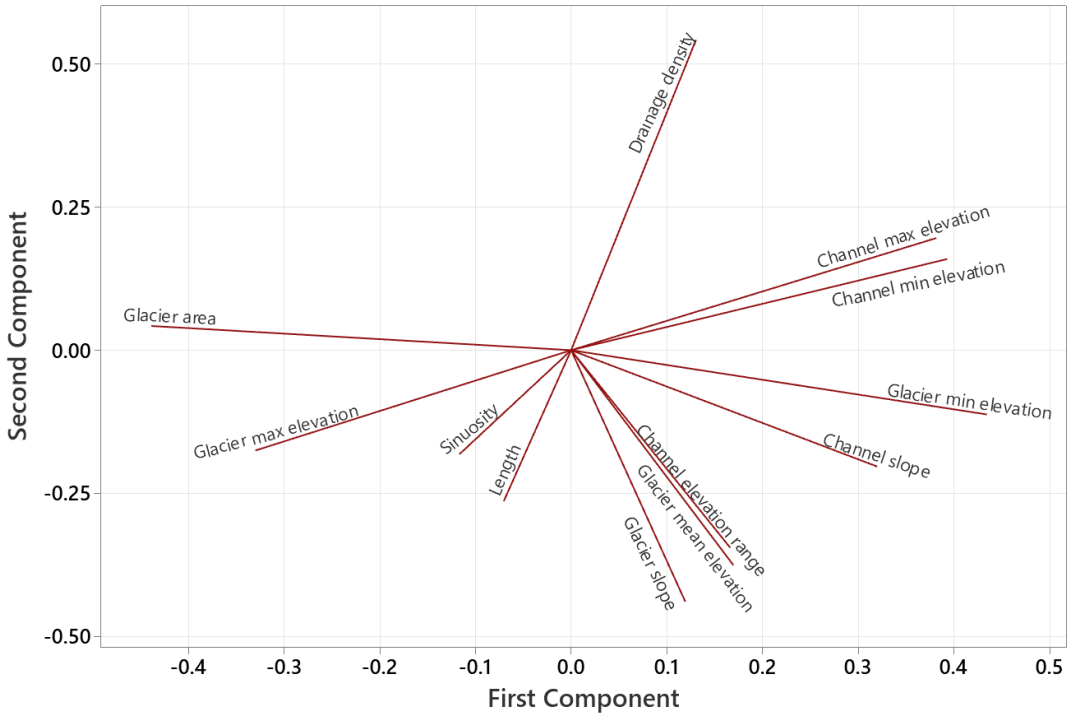

Figure S1: loading plot for principal components 1 and 2 from a PCA analysis of glacier and channel characteristics.

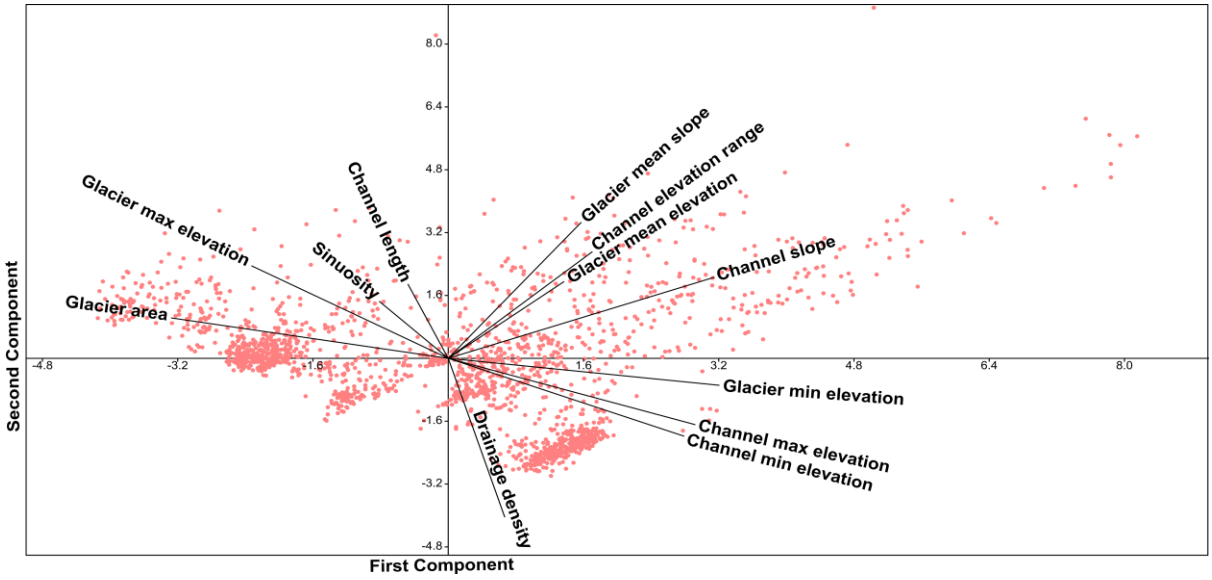

Figure S2: A biplot from a PCA analysis showing principal components 1 and 2, which was used for cluster analysis and overlayed with a loading plot (see Fig. S1).

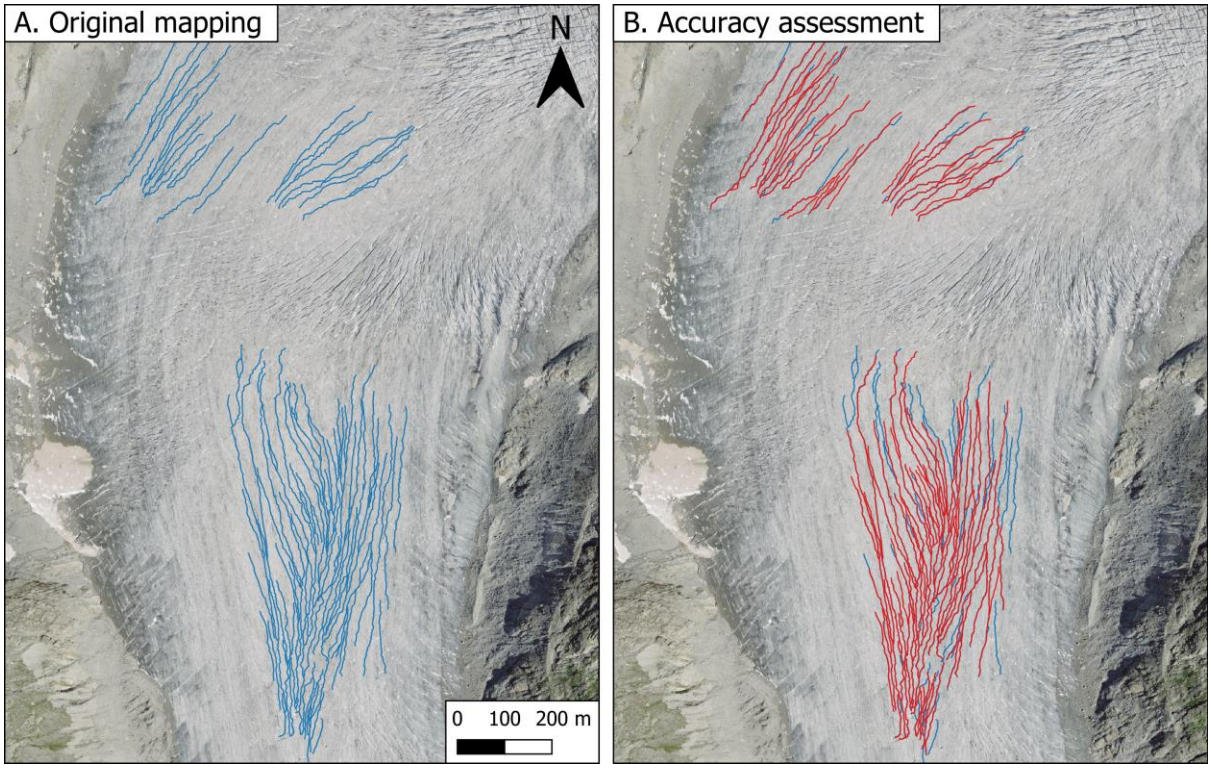

Figure S3: Repeat mapping of the Rhonegletscher used to determine mapping accuracy. (A) Mapping from this dataset is shown in blue. (B) A comparison between the repeat mapping (red) and the original mapping (blue), which was undertaken independently after several weeks had elapsed.

Data availability

The orthophoto and DEM data used in this study are freely available on the SwissTopo website (https://www.swisstopo.admin.ch/). Outlines of glaciers in Valais were obtained from Glacier Monitoring in Switzerland (GLAMOS) and are available online (https://glamos.ch/). The produced supraglacial channel data is available upon request from the corresponding author (Holly Wytiahlowsky: holly.e.wytiahlowsky@durham.ac.uk).

Author contributions

All authors contributed to the conceptualisation of this project. HW conducted the mapping, formal analysis and data visualisation under the supervision of CRS, RAH, CCC and SSRJ. HW led manuscript writing with comments and revisions provided by all authors.

Competing interests

CC is a member of the editorial board of The Cryosphere and CRS was a member at the time of submission.

Acknowledgements

This work was supported by the Natural Environment Research Council via an IAPETUS2 PhD studentship held by Holly Wytiahlowsky (grant reference NE/S007431/1). We thank SwissTopo for making their orthophotos and DEM data open access. We thank two anonymous reviewers and Ian Willis for their constructive feedback which has helped to improve this paper, and Kang Yang for acting as editor for the manuscript.

8 References

Bamber, J. L., Oppenheimer, M., Kopp, R. E., Aspinall, W. P., and Cooke, R. M.: Ice sheet contributions to future sea-level rise from structured expert judgment, Proc. Natl. Acad. Sci., 116, 11195–11200, doi:10.1073/pnas.1817205116, 2019.

Banwell, A., Hewitt, I., Willis, I., and Arnold, N.: Moulin density controls drainage development beneath the Greenland ice sheet, J. Geophys. Res. Earth Surf., 121, 2248–2269, doi:10.1002/2015JF003801, 2016.

Bell, R. E., Chu, W., Kingslake, J., Das, I., Tedesco, M., Tinto, K. J., Zappa, C. J., Frezzotti, M., Boghosian, A., and Lee, W. S.: Antarctic ice shelf potentially stabilized by export of meltwater in surface river, Nature, 544, 344–348, doi:10.1038/nature22048, 2017.

Benn, D. I., Thompson, S., Gulley, J., Mertes, J., Luckman, A., and Nicholson, L.: Structure and evolution of the drainage system of a Himalayan debris-covered glacier, and its relationship with patterns of mass loss, Cryosphere, 11, 2247–2264, doi:10.5194/tc-11-2247-2017, 2017.

Carey, M., Molden, O. C., Rasmussen, M. B., Jackson, M., Nolin, A. W., and Mark, B. G.: Impacts of glacier recession and declining meltwater on mountain societies, Ann. Am. Assoc. Geogr., 107, 350–359, doi:10.1080/24694452.2016.1243039, 2017.

Chen, J., Hodge, R.A., Jamieson, S.S.R. and Stokes, C.R.: Distribution and morphometry of supraglacial channel networks on Antarctic ice shelves. J. Glaciol., doi:10.1017/jog.2024.99, 2024.

Chu, V. W.: Greenland Ice Sheet hydrology: A review, Prog. Phys. Geogr., 38, 19–54, doi:10.1177/0309133313507075, 2014.

Chudley, T. R., Christoffersen, P., Doyle, S. H., Bougamont, M., Schoonman, C. M., Hubbard, B., and James, M. R.: Supraglacial lake drainage at a fast-flowing Greenlandic outlet glacier, Proc. Natl. Acad. Sci., 116, 25468–25477, doi:10.1073/pnas.1913685116, 2019.

Chudley, T. R., Christoffersen, P., Doyle, S. H., Dowling, T. P. F., Law, R., Schoonman, C. M., Bougamont, M., and Hubbard, B.: Controls on Water Storage and Drainage in Crevasses on the Greenland Ice Sheet, J. Geophys. Res. Earth Surf., 126, e2021JF006287, doi:10.1029/2021JF006287, 2021.

Clason, C., Rangecroft, S., Owens, P. N., Łokas, E., Baccolo, G., Selmes, N., Beard, D., Kitch, J., Dextre, R. M., Morera, S., and Blake, W.: Contribution of glaciers to water, energy and food security in mountain regions: current perspectives and future priorities, Ann. Glaciol., 63, 73–78, doi:10.1017/aog.2023.14, 2023.

Das, S. B., Joughin, I., Behn, M. D., Howat, I. M., King, M. A., Lizarralde, D., and Bhatia, M. P.: Fracture propagation to the base of the Greenland Ice Sheet during supraglacial lake drainage, Science, 320, 778–781, doi:10.1126/science.1153360, 2008.

Davaze, L., Rabatel, A., Dufour, A., Hugonnet, R., and Arnaud, Y.: Region-wide annual glacier surface mass balance for the European Alps from 2000 to 2016, Front. Earth Sci., 8, doi:10.3389/feart.2020.00149, 2020.

Delaney, I. and Adhikari, S.: Increased subglacial sediment discharge in a warming climate: consideration of ice dynamics, glacial erosion, and fluvial sediment transport, Geophys. Res. Lett., 47, e2019GL085672, doi:10.1029/2019GL085672, 2020.

Dozier, J.: An examination of the variance minimization tendencies of a supraglacial stream, J. Hydrol., 31, 359–380, doi:10.1016/0022-1694(76)90134-7, 1976.

Edwards, T. L., Nowicki, S., Marzeion, B., Hock, R., Goelzer, H., Seroussi, H., Jourdain, N. C., Slater, D. A., Turner, F. E., Smith, C. J., McKenna, C. M., Simon, E., Abe-Ouchi, A., Gregory, J. M., Larour, E., Lipscomb, W. H., Payne, A. J., Shepherd, A., Agosta, C., Alexander, P., Albrecht, T., Anderson, B., Asay-Davis, X., Aschwanden, A., Barthel, A., Bliss, A., Calov, R., Chambers, C., Champollion, N., Choi, Y., Cullather, R., Cuzzone, J., Dumas, C., Felikson, D., Fettweis, X., Fujita, K., Galton-Fenzi, B. K., Gladstone, R., Golledge, N. R., Greve, R., Hattermann, T., Hoffman, M. J., Humbert, A., Huss, M., Huybrechts, P., Immerzeel, W., Kleiner, T., Kraaijenbrink, P., Le clec'h, S., Lee, V., Leguy, G. R., Little, C. M., Lowry, D. P., Malles, J.-H., Martin, D. F., Maussion, F., Morlighem, M., O'Neill, J. F., Nias, I., Pattyn, F., Pelle, T., Price, S. F., Quiquet, A., Radić, V., Reese, R., Rounce, D. R., Rückamp, M., Sakai, A., Shafer, C., Schlegel, N.-J., Shannon, S., Smith, R. S., Straneo, F., Sun, S., Tarasov, L., Trusel, L. D., Van Breedam, J., van de Wal, R., van den Broeke, M., Winkelmann, R., Zekollari, H., Zhao, C., Zhang, T., and Zwinger, T.: Projected land ice contributions to twenty-first-century sea level rise, Nature, 593, 74–82, doi:10.1038/s41586-021-03302-y, 2021.

Esri. "Imagery" [basemap]. Scale Not Given. "World Imagery". October 10, 2024. https://www.arcgis.com/home/item.html?id=10df2279f9684e4a9f6a7f08febac2a9. (October 22, 2024)

Ferguson, R. I.: Sinuosity of supraglacial streams, Geol. Soc. Am. Bull., 84, 251–256, doi:10.1130/0016-7606(1973)84<251:SOSS>2.0.CO;2, 1973.

Fischer, M., Huss, M., and Hoelzle, M.: Surface elevation and mass changes of all Swiss glaciers 1980–2010, Cryosphere, 9, 525–540, doi:10.5194/tc-9-525-2015, 2015.

Fleischer, F., Otto, J.-C., Junker, R. R., and Hölbling, D.: Evolution of debris cover on glaciers of the Eastern Alps, Austria, between 1996 and 2015, Earth Surf. Process. Landf., 46, 1673–1691, doi:10.1002/esp.5065, 2021.

Fyffe, C. L., Brock, B. W., Kirkbride, M. P., Mair, D. W. F., Arnold, N. S., Smiraglia, C., Diolaiuti, G., and Diotri, F.: Do debris-covered glaciers demonstrate distinctive hydrological behaviour compared to clean glaciers?, J. Hydrol., 570, 584–597, doi:10.1016/j.jhydrol.2018.12.069, 2019.

Glasser, N. F., Holt, T. O., Evans, Z. D., Davies, B. J., Pelto, M., and Harrison, S.: Recent spatial and temporal variations in debris cover on Patagonian glaciers, Geomorphology, 273, 202–216, doi:10.1016/j.geomorph.2016.07.036, 2016.

Gleason, C. J., Smith, L. C., Chu, V. W., Legleiter, C. J., Pitcher, L. H., Overstreet, B. T., Rennermalm, A. K., Forster, R. R., and Yang, K.: Characterizing supraglacial meltwater channel hydraulics on the Greenland Ice Sheet from in situ observations, Earth Surf. Process. Landf., 41, 2111–2122, doi:10.1002/esp.3977, 2016.

Gleason, C. J., Yang, K., Feng, D., Smith, L. C., Liu, K., Pitcher, L. H., Chu, V. W., Cooper, M. G., Overstreet, B. T., Rennermalm, A. K., and Ryan, J. C.: Hourly surface meltwater routing for a Greenlandic supraglacial catchment across hillslopes and through a dense topological channel network, Cryosphere, 15, 2315–2331, doi:10.5194/tc-15-2315-2021, 2021.

Gulley, J. D., Benn, D. I., Mueller, D., and Luckman, A.: A cut-and-closure origin for englacial conduits in uncrevassed regions of polythermal glaciers, J. Glaciol., 55, 66–80, doi:10.3189/002214309788608930, 2009.

Hambrey, M. J.: Supraglacial drainage and its relationship to structure, with particular reference to Charles Rabots Bre, Okstindan, Norway, Nor. Geogr. Tidsskr., 31, 69–77, doi:10.1080/00291957708545319, 1977.

Horton, R. E.: Erosional development of streams and their drainage basins; hydrophysical approach to quantitative morphology, Geol. Soc. Am. Bull., 56, 275–370, doi:10.1130/0016-7606(1945)56[275:EDOSAT]2.0.CO;2, 1945.

Hugonnet, R., McNabb, R., Berthier, E., Menounos, B., Nuth, C., Girod, L., Farinotti, D., Huss, M., Dussaillant, I., Brun, F., and Kääb, A.: Accelerated global glacier mass loss in the early twenty-first century, Nature, 592, 726–731, doi:10.1038/s41586-021-03436-z, 2021.

Huss, M., Bauder, A., Werder, M., Funk, M., and Hock, R.: Glacier-dammed lake outburst events of Gornersee, Switzerland, J. Glaciol., 53, 189–200, doi.org:10.3189/172756507782202784, 2007.

Immerzeel, W. W., Lutz, A. F., Andrade, M., Bahl, A., Biemans, H., Bolch, T., Hyde, S., Brumby, S., Davies, B. J., Elmore, A. C., Emmer, A., Feng, M., Fernández, A., Haritashya, U., Kargel, J. S., Koppes, M., Kraaijenbrink, P. D. A., Kulkarni, A. V., Mayewski, P. A., Nepal, S., Pacheco, P., Painter, T. H., Pellicciotti, F., Rajaram, H., Rupper, S., Sinisalo, A., Shrestha, A. B., Viviroli, D., Wada, Y., Xiao, C., Yao, T., and Baillie, J. E. M.: Importance and vulnerability of the world's water towers, Nature, 577, 364–369, doi:10.1038/s41586-019-1822-y, 2020.

Irvine-Fynn, T. D. L., Hodson, A. J., Moorman, B. J., Vatne, G., and Hubbard, A. L.: Polythermal glacier hydrology: a review, Rev. Geophys., 49, doi:10.1029/2010RG000350, 2011.

Jobard, S. and Dzikowski, M.: Evolution of glacial flow and drainage during the ablation season, J. Hydrol., 330, 663–671, doi:10.1016/j.jhydrol.2006.04.031, 2006.

Karlstrom, L. and Yang, K.: Fluvial supraglacial landscape evolution on the Greenland Ice Sheet, Geophys. Res. Lett., 43, 2683–2692, doi:10.1002/2016GL067697, 2016.

Khan, A. L., Xian, P., and Schwarz, J. P.: Black carbon concentrations and modeled smoke deposition fluxes to the bare-ice dark zone of the Greenland Ice Sheet, Cryosphere, 17, 2909–2918, doi:10.5194/tc-17-2909-2023, 2023.

King, L., Hassan, M. A., Yang, K., and Flowers, G.: Flow routing for delineating supraglacial meltwater channel networks, Remote Sens., 8, 988, doi:10.3390/rs8120988, 2016.

Kingslake, J., Ely, J. C., Das, I., and Bell, R. E.: Widespread movement of meltwater onto and across Antarctic ice shelves, Nature, 544, 349–352, doi:10.1038/nature22049, 2017.

Knighton, A. D.: Channel form adjustment in supraglacial streams, Austre Okstindbreen, Norway, Arct. Antarct. Alp. Res., 17, 451, doi:10.2307/1550870, 1985.

Knighton, A. D.: Channel form and flow characteristics of supraglacial streams, Austre Okstindbreen, Norway, Arct. Alp. Res., 13, 295, doi:10.2307/1551036, 1981.

Knighton, A. D.: Meandering habit of supraglacial streams, Geol. Soc. Am. Bull., 83, 201–204, doi:10.1130/0016-7606(1972)83[201:MHOSS]2.0.CO;2, 1972.

Leeson, A. A., Shepherd, A., Briggs, K., Howat, I., Fettweis, X., Morlighem, M., and Rignot, E.: Supraglacial lakes on the Greenland Ice Sheet advance inland under warming climate, Nat. Clim. Change, 5, 51–55, doi:10.1038/nclimate2463, 2015.

Leidman, S. Z., Rennermalm, Å. K., Muthyala, R., Guo, Q., and Overeem, I.: The presence and widespread distribution of dark sediment in Greenland Ice Sheet supraglacial streams implies substantial impact of microbial communities on sediment deposition and albedo, Geophys. Res. Lett., 48, 2020GL088444, doi:10.1029/2020GL088444, 2021.

Leigh, J. R., Stokes, C. R., Carr, R. J., Evans, I. S., Andreassen, L. M., and Evans, D. J. A.: Identifying and mapping very small (<0.5 km^2) mountain glaciers on coarse to high-resolution imagery, J. Glaciol., 65, 873–888, https://doi.org/10.1017/jog.2019.50, 2019.

Leinss, S. and Bernhard, P.: TanDEM-X:Deriving InSAR height changes and velocity dynamics of Great Aletsch Glacier, IEEE J. Sel. Top. Appl. Earth Obs. Remote Sens., 14, 4798–4815, https://doi.org/10.1109/JSTARS.2021.3078084, 2021.

Linsbauer, A., Huss, M., Hodel, E., Bauder, A., Fischer, M., Weidmann, Y., Bärtschi, H., and Schmassmann, E.: The new Swiss glacier inventory SGI2016: from a topographical to a glaciological dataset, Front. Earth Sci., 9, doi:10.3389/feart.2021.704189, 2021.

Mantelli, E., Camporeale, C., and Ridolfi, L.: Supraglacial channel inception: modeling and processes, Water Resour. Res., 51, 7044–7063, doi:10.1002/2015WR017075, 2015.

Marston, R. A.: Supraglacial stream dynamics on the Juneau Icefield, Ann. Am. Assoc. Geogr., 73, 597–608, doi:10.1111/j.1467-8306.1983.tb01861.x, 1983.

MeteoSwiss: https://www.meteoswiss.admin.ch/, last access: 1 February 2024.

Micheletti, N. and Lane, S. N.: Water yield and sediment export in small, partially glaciated Alpine watersheds in a warming climate, Water Resour. Res., 52, 4924–4943, doi: 10.1002/2016WR018774, 2016.

Mölg, N., Bolch, T., Walter, A., and Vieli, A.: Unravelling the evolution of Zmuttgletscher and its debris cover since the end of the Little Ice Age, Cryosphere, 13, 1889–1909, doi:10.5194/tc-13-1889-2019, 2019.

Moore, R. C.: Origin of Inclosed Meanders on Streams of the Colorado Plateau, J. Glaciol., 34, 29–57, doi:10.1086/623270, 1926.

Morriss, B. F., Hawley, R. L., Chipman, J. W., Andrews, L. C., Catania, G. A., Hoffman, M. J., Lüthi, M. P., and Neumann, T. A.: A ten-year record of supraglacial lake evolution and rapid drainage in West Greenland using an automated processing algorithm for multispectral imagery, Cryosphere, 7, 1869–1877, doi:10.5194/tc-7-1869-2013, 2013.

Nienow, P., Sharp, M., and Willis, I.: Seasonal changes in the morphology of the subglacial drainage system, Haut Glacier d'Arolla, Switzerland, Earth Surf. Process. Landf., 23, 825–843, https://doi.org/10.1002/(SICI)1096-9837(199809)23:9<825::AID-ESP893>3.0.CO;2-2, 1998.

Pitcher, L. H. and Smith, L. C.: Supraglacial Streams and Rivers, Annu. Rev. Earth Planet. Sci., 47, 421–452, doi:10.1146/annurev-earth-053018-060212, 2019.

Rippin, D. M., Pomfret, A., and King, N.: High resolution mapping of supra-glacial drainage pathways reveals link between micro-channel drainage density, surface roughness and surface reflectance, Earth Surf. Process. Landf., 40, 1279–1290, doi:10.1002/esp.3719, 2015.

Rounce, D. R., Hock, R., Maussion, F., Hugonnet, R., Kochtitzky, W., Huss, M., Berthier, E., Brinkerhoff, D., Compagno, L., Copland, L., Farinotti, D., Menounos, B., and McNabb, R. W.: Global glacier change in the 21st century: Every increase in temperature matters, Science, 379, 78–83, doi:10.1126/science.abo1324, 2023.

Ryan, J. C., Hubbard, A., Stibal, M., Irvine-Fynn, T. D., Cook, J., Smith, L. C., Cameron, K., and Box, J.: Dark zone of the Greenland Ice Sheet controlled by distributed biologically-active impurities, Nat. Commun., 9, 1065, doi:10.1038/s41467-018-03353-2, 2018.

Seaberg, S. Z., Seaberg, J. Z., Hooke, R. L., and Wiberg, D. W.: Character of the englacial and subglacial drainage system in the lower part of the ablation area of Storglaciären, Sweden, as Revealed by Dye-Trace Studies, J. Glaciol., 34, 217–227, doi:10.3189/S0022143000032263, 1988.

Shepherd, R. G.: Incised river meanders: evolution in simulated bedrock, Science, 178, 409–411, doi:10.1126/science.178.4059.409, 1972.

Smith, L. C., Chu, V. W., Yang, K., Gleason, C. J., Pitcher, L. H., Rennermalm, A. K., Legleiter, C. J., Behar, A. E., Overstreet, B. T., Moustafa, S. E., Tedesco, M., Forster, R. R., LeWinter, A. L., Finnegan, D. C., Sheng, Y., and Balog, J.: Efficient meltwater drainage through supraglacial streams and rivers on the southwest Greenland Ice Sheet, Proc. Natl. Acad. Sci., 112, 1001–1006, doi:10.1073/pnas.1413024112, 2015.

Sommer, C., Malz, P., Seehaus, T. C., Lippl, S., Zemp, M., and Braun, M. H.: Rapid glacier retreat and downwasting throughout the European Alps in the early 21st century, Nat. Commun., 11, 3209, doi:10.1038/s41467-020-16818-0, 2020.

St Germain, S. L. and Moorman, B. J.: Long-term observations of supraglacial streams on an Arctic glacier, J. Glaciol., 65, 900–911, doi:10.1017/jog.2019.60, 2019.

Swift, D. A., Nienow, P. W., Spedding, N., and Hoey, T. B.: Geomorphic implications of subglacial drainage configuration: rates of basal sediment evacuation controlled by seasonal drainage system evolution, Sediment. Geol., 149, 5–19, doi:10.1016/S0037-0738(01)00241-X, 2002.

Tepes, P., Gourmelen, N., Nienow, P., Tsamados, M., Shepherd, A., and Weissgerber, F.: Changes in elevation and mass of Arctic glaciers and ice caps, 2010–2017, Remote Sens. Environ., 261, 112481, doi:10.1016/j.rse.2021.112481, 2021.

The GlaMBIE Team: Community estimate of global glacier mass changes from 2000 to 2023, Nature, 1–7, doi:10.1038/s41586-024-08545-z, 2025.

Turowski, J. M.: Alluvial cover controlling the width, slope and sinuosity of bedrock channels, Earth Surf. Dyn., 6, 29–48, doi:10.5194/esurf-6-29-2018, 2018.

Willis, I.C.: Intra-annual variations in glacier motion: a review, Prog. Phys. Geogr., 19. doi:10.1177/030913339501900104, 1995.

Wouters, B., Gardner, A. S., and Moholdt, G.: Global glacier mass loss during the GRACE satellite mission (2002-2016), Front. Earth Sci., 7, 2019.

Yang, K. and Smith, L. C.: Internally drained catchments dominate supraglacial hydrology of the southwest Greenland Ice Sheet, J. Geophys. Res.-Earth Surf., 121, doi:10.1002/2016JF003927, 2016.

Yang, K. and Smith, L. C.: Supraglacial streams on the Greenland Ice Sheet delineated from combined spectral-shape information in high-resolution satellite imagery, IEEE Geosci. Remote Sens. Lett., 10, 801–805, doi:10.1109/LGRS.2012.2224316, 2013.

Yang, K., Smith, L. C., Andrews, L. C., Fettweis, X., and Li, M.: Supraglacial drainage efficiency of the Greenland Ice Sheet estimated from remote sensing and climate models, J. Geophys. Res.-Earth Surf., 127, e2021JF006269, doi:10.1029/2021JF006269, 2022.

Yang, K., Smith, L. C., Chu, V. W., Gleason, C. J., and Li, M.: A caution on the use of surface digital elevation models to simulate supraglacial hydrology of the Greenland Ice Sheet, IEEE J. Sel. Top. Appl. Earth Observ. Remote Sens., 8, 5212–5224, doi:10.1109/JSTARS.2015.2483483, 2015.

Yang, K., Smith, L. C., Chu, V. W., Pitcher, L. H., Gleason, C. J., Rennermalm, A. K., and Li, M.: Fluvial morphometry of supraglacial river networks on the southwest Greenland Ice Sheet, GISci. Remote Sens., 53, 459–482, doi:10.1080/15481603.2016.1162345, 2016.

Yang, K., Smith, L. C., Cooper, M. G., Pitcher, L. H., As, D. van, Lu, Y., Lu, X., and Li, M.: Seasonal evolution of supraglacial lakes and rivers on the southwest Greenland Ice Sheet, J. Glaciol., 67, 592–602, doi:10.1017/jog.2021.10, 2021.

Yang, K., Smith, L. C., Karlstrom, L., Cooper, M. G., Tedesco, M., van As, D., Cheng, X., Chen, Z., and Li, M.: A new surface meltwater routing model for use on the Greenland Ice Sheet surface, Cryosphere, 12, 3791–3811, doi:10.5194/tc-12-3791-2018, 2018.

Yang, K., Smith, L. C., Sole, A., Livingstone, S. J., Cheng, X., Chen, Z., and Li, M.: Supraglacial rivers on the northwest Greenland Ice Sheet, Devon Ice Cap, and Barnes Ice Cap mapped using Sentinel-2 imagery, Int. J. Appl. Earth Obs. Geoinf., 78, 1–13, doi:10.1016/j.jag.2019.01.008, 2019.

Yang, K., Sommers, A., Andrews, L. C., Smith, L. C., Lu, X., Fettweis, X., and Li, M.: Intercomparison of surface meltwater routing models for the Greenland Ice Sheet and influence on subglacial effective pressures, Cryosphere, 14, 3349–3365, doi:10.5194/tc-14-3349-2020, 2020.

Zekollari, H., Huss, M., and Farinotti, D.: Modelling the future evolution of glaciers in the European Alps under the EURO-CORDEX RCM ensemble, Cryosphere, 13, 1125–1146, doi:10.5194/tc-13-1125-2019, 2019.

Zemp, M., Huss, M., Thibert, E., Eckert, N., McNabb, R., Huber, J., Barandun, M., Machguth, H., Nussbaumer, S. U., Gärtner-Roer, I., Thomson, L., Paul, F., Maussion, F., Kutuzov, S., and Cogley, J. G.: Global glacier mass changes and their contributions to sea-level rise from 1961 to 2016, Nature, 568, 382–386, doi:10.1038/s41586-019-1071-0, 2019.